ID	Dual-tropic		CXCR4-tropic		CCR5-tropic				mean ID50 (% neutralization)
	29CC1	41CC1	98CC2	107CC2	47CC11	55PL1	102CC2	105PL3	
R1	89					291	27		136 (38%)
R2	198			154		297		637	322 (50%)
R3	319			21		175	151		167 (50%)
R4	127								127 (13%)
R5	56								56 (13%)
R6	180	104	36	153		325	54		142 (75%)
R7		228		93		35	33		97 (50%)
R8									0 (0%)
R9	35	50		141		832		60	224 (63%)
R10	83	57		58					66 (38%)
R11	60								60 (13%)
R12									0 (0%)
R13	63	132		325		70	90	72	125 (75%)
R14						63			63 (13%)
R15						73			73 (13%)
R16	326		26	145		768	51	108	237 (75%)
R17	25					1065			545 (25%)
R18	184			60		61			102 (38%)
R19	69			197		178			148 (38%)
R20						59		28	44 (25%)
R21	572			244					408 (25%)
R22	114			48					81 (25%)
R23	496	52		1332	27	1413	34	63	488 (88%)
R24	309	488	44	796			295	163	349 (75%)
R25	542			29		2317		140	757 (50%)
R26	308	54	82	190		1220	178	90	303 (88%)
R27	56			76					66 (25%)
R28	218			804	74	64			315 (50%)
R29	118			77				21	72 (38%)
R30	153	38		170	154	585	78	198	197 (88%)
R31						60		25	43 (25%)
R32	169			246				55	157 (38%)
R33	40			52		63		32	47 (50%)
mean ID50 (% neutralization)	189 (79%)	134 (27%)	47 (12%)	251 (67%)	85 (9%)	477 (64%)	99 (30%)	121 (42%)	

ID50 > 500
500 > ID50 > 100
100 > ID50 > 20
no neutralization

Figure 1. Anti-HIV-1 neutralizing activity of plasma derived from 33 rapid progressors against AE-Env-recombinant viruses. Neutralizing activity of plasma samples against 8 AE-Env-recombinant viruses was evaluated and reciprocal plasma dilution at which viral replication was suppressed by 50% (50% inhibitory dilution, ID50) was calculated, as described in Methods. Data are presented as the means of at least three independent experiments. Plasma IDs and AE-Env-recombinant viruses tested are denoted on the left side and above the panel, respectively. In addition, mean ID50 values and the percentages of virus/plasma combinations (% neutralization) in which viral neutralization was observed among the data sets in horizontal and vertical directions are shown on the right side and bottom of the panel, respectively. ID50 values >500, values 100–500, and values 20–100 are highlighted in red, orange and yellow, respectively. In addition, no neutralization (ID50 values <20) of a recombinant virus is denoted by a gray background.
doi:10.1371/journal.pone.0053920.g001

ing how such neutralizing antibodies are elicited in infected patients may provide valuable insights into developing an effective HIV-1 vaccine.

HIV-1 is characterized by extensive genetic heterogeneity and is divided into four groups: M (major), O (outlying), N (new or non-M, non-O) and P (pending). The viruses in group M, which are responsible for the worldwide HIV-1 pandemic, are further classified into many subtypes and circulating recombinant forms (CRFs) [9]. While subtype B of HIV-1 is the predominant subtype in the Americas, Europe and Australia, there is a growing epidemic of non-B subtypes and CRFs in Africa and Asia. CRF01_AE is prevalent throughout Southeast Asia [9] and is responsible for more than 80% of infection cases in Thailand [10].

In this report, as part of studies to reveal the molecular mechanism of how strong humoral immune responses are elicited in HIV-1-infected patients, we performed a comparative study on the neutralizing activity of plasma derived from rapid and slow progressors residing in northern Thailand, using previously established high throughput neutralization tests with CRF01_AE Env-recombinant, luciferase reporter viruses [11,12].

Methods

Ethics statement

This study was conducted with approval from the ethics committee of the Ministry of Public Health of Thailand and with written informed consent from the patients.

Study participants and sample collection

We studied plasma samples of drug-naive, HIV-1-infected patients who visited the day care center of Lampang Hospital in the early to middle 2000 s, and who were enrolled in a HIV-1 cohort study. Thirty-four plasma samples were derived from slow progressors (CD4 count >100 cells/cm^3 at the time of enrollment, healthy for at least 8 years without antiretroviral treatment), whereas 33 plasma samples were derived from rapid progressors (CD4 count >100 cells/cm^3 at the time of enrollment, died with AIDS symptoms within 5 years). Plasma samples were heat-inactivated for 1 hr at 56°C and subjected to neutralization tests.

Cells

293T cells were maintained in Dulbecco's modified Eagle's medium supplemented with 10% fetal bovine serum (10% FBS-

ID	Dual-tropic		CXCR4-tropic		CCR5-tropic				mean ID50 (% neutralization)
	29CC1	41CC1	98CC2	107CC2	47CC11	55PL1	102CC2	105PL3	
S1	204					492			348 (25%)
S2	44	53		21		175	151		89 (63%)
S3	55								55 (13%)
S4	42								42 (13%)
S5	46	22							34 (25%)
S6	60					776			418 (25%)
S7	122	52	49	572	27	1411	78	272	323 (100%)
S8	69								69 (13%)
S9	29								29 (13%)
S10	147								147 (13%)
S11	151					34			93 (25%)
S12	34			32					33 (25%)
S13	203		29	61		66		101	92 (63%)
S14									0 (0%)
S15	63		62	205	37	511	116	41	148 (88%)
S16									0 (0%)
S17						255			255 (13%)
S18									0 (0%)
S19	191					108	43	32	94 (50%)
S20									0 (0%)
S21	217							108	163 (25%)
S22	157		112			137			135 (38%)
S23	34	57	28	988	23	898	57	252	292 (100%)
S24									0 (0%)
S25						52			52 (13%)
S26				66		45			56 (25%)
S27				31		22			27 (25%)
S28	113	53		246	70	496	112	45	162 (88%)
S29	221			83				43	116 (38%)
S30	419	45	65	186		55	40	302	159 (88%)
S31	168	257	293	524	100	278	100	355	259 (100%)
S32	717			36				71	275 (38%)
S33	340							72	206 (25%)
S34	1281	72	27	1518	35	116	23	448	440 (100%)
mean ID50 (% neutralization)	205 (74%)	76 (24%)	83 (24%)	326 (41%)	49 (18%)	329 (53%)	80 (26%)	165 (38%)	

ID50 > 500
500 > ID50 > 100
100 > ID50 > 20
no neutralization
plasma that neutralized all AE-Env-recombinant viruses tested

Figure 2. Anti-HIV-1 neutralizing activity of plasma derived from 34 slow progressors against AE-Env-recombinant viruses. Neutralizing activity of plasma samples against 8 AE-Env-recombinant viruses was evaluated as described in the legend to Figure 1. Data are presented as the means of at least three independent experiments. Plasma IDs and AE-Env-recombinant viruses tested are denoted on the left side and above the panel, respectively. In addition, mean ID50 values and the percentages of virus/plasma combinations (% neutralization) in which viral neutralization was observed among the data sets in horizontal and vertical directions are shown on the right side and bottom of the panel, respectively. ID50 values >500, values 100–500 and values 20–100 are highlighted in red, orange and yellow, respectively. No neutralization (ID50 values <20) of a recombinant virus is denoted by a gray background. Plasma samples that neutralized all recombinant viruses tested are highlighted in green.
doi:10.1371/journal.pone.0053920.g002

DMEM). U87.CD4.CCR5 and U87.CD4.CXCR4 cells [13] were obtained from Dr. HongKui Deng and Dr. Dan R. Littman through the AIDS Research and Reference Reagent Program (ARRRP), Division of AIDS, NIAID, NIH, and were maintained in 10% FBS-DMEM with puromycin (1 μg/ml) and G418 (300 μg/ml) (complete medium).

Viral constructs

CRF01_AE-Env (AE-Env)-recombinant, luciferase reporter proviral constructs containing the CRF01_AE *env* genes, 29CC1, 41CC1, 47CC1, 55PL1, 98CC2, 102CC2 and 105PL3, were generated as described previously [12]. The expression vectors for 5 subtype B Env (B-Env), QH0692.42, TRO.11, pWITO4160.33, pREJO4541.67 and SC422661.8 [14,15,16], and the vectors for 6 subtype C Env (C-Env), ZM214M.PL15, ZM249MPL1, ZM53M.PB12, ZM109F.PB4, ZM135M.PL10a and CAP210.2.00.E8 [17], were obtained from Drs. Cynthia A. Derdeyn, Feng Gao, Beatrice H. Hahn, Eric Hunter, Ming Li, Yingying Li, Koleka Milsana, David C. Montefiori, Lynn Morris and Jesus F. Salazar-Gonzalez through the ARRRP. Subtype B and C *env* genes were amplified from these expression vectors by polymerase chain reaction and inserted into pNL4-3-derived luciferase reporter viral DNA, pNL-envCT to generate B-Env- and C-Env-recombinant, luciferase reporter proviral constructs, essentially as described [12,18].

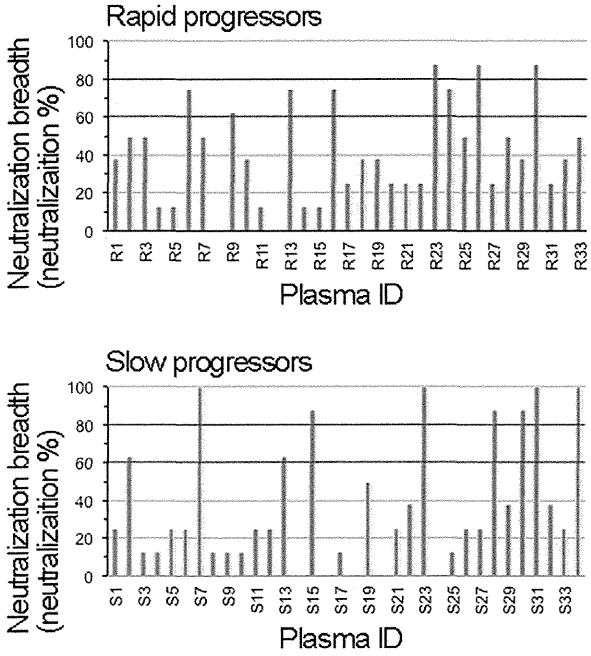

Figure 3. Comparison of the neutralization breadth between plasma derived from rapid and slow progressors. The proportion of AE-Env-recombinant viruses in which replication was inhibited by a plasma sample was calculated and plotted. The levels of plasma-mediated neutralization against 60% and 80% of recombinant viruses tested are highlighted by horizontal blue and red grid lines, respectively. Plasma IDs are denoted below the panels.
doi:10.1371/journal.pone.0053920.g003

Preparation of Env-recombinant viruses

293T cells (2×10^5 cells/2 ml) were seeded onto a collagen-coated 6-well plate (Iwaki, Tokyo, Japan) 24 h prior to transfection. Env-recombinant viruses were prepared by transfecting 293T cells with a proviral construct (2 μg) using FuGENE HD transfection reagent (Roche, Basel, Switzerland). Forty-eight hours after transfection, viral supernatants were cleared by centrifugation for 5 min at 8,000 rpm and stored as aliquots at −85°C. The viral titer was determined by measuring the concentration of HIV-1 Gag p24 antigen in viral supernatants by enzyme-linked immunosorbent assay (ELISA) (HIV-1 p24 ELISA Kit; BioAcademia, Inc., Osaka, Japan).

Neutralization tests

The neutralization susceptibility of Env-recombinant viruses to plasma samples was examined, essentially as described previously [11]. Briefly, U87.CD4.CXCR4 or U87.CD4.CCR5 cells were incubated with 2-fold serially diluted plasma in 100 μl complete medium for 1 hr at 37°C. U87.CD4.CXCR4 cells were used as target cells for recombinant viruses containing CXCR4-tropic AE-Env, 98CC2 and 107CC2, and dual-tropic AE-Env, 29CC1 and 41CC1. In addition, U87.CD4.CCR5 cells were used as target cells for recombinant viruses containing CCR5-tropic AE-Env, 47CC11, 55PL1, 102CC2 and 105PL3, 2 dual-tropic AE-Env, 5 B-Env and 6 C-Env. The cells were then incubated with viral supernatants (2 ng of p24 antigen) for 48 hrs. Luciferase activity in infected cells was measured using the Steady Glo Luciferase assay kit (Promega) with an LB960 microplate luminometer (Berthold, Bad Wildbad, Germany). The inhibitory effect of the plasma on viral replication was evaluated as a reduction in luciferase activity in infected cells. The reciprocal plasma dilution, at which viral replication was suppressed by 50% (50% inhibitory dilution, ID50), was calculated by the dose-response curve using a standard function of GraphPad Prism 5 software (GraphPad Software, San Diego, CA).

Statistical analyses

Fisher's exact test was performed to compare the breadth of neutralizing activity in plasma derived from rapid and slow progressors. Briefly, a 2×2 contingency table, consisting of the numbers of plasma/virus combinations in which viral neutralization was observed and total plasma/virus combinations on both groups, was constructed, and the 2-tailed p-value was calculated using QuickCalcs (GraphPad software; http://www.graphpad.com/quickcalcs/). In addition, Student' t-test was performed to compare the potency of neutralizing plasmas derived from rapid and slow progressors, using the standard function of Microsoft Excel (Microsoft Office for Mac 2011; Microsoft, Redmond, WA).

ID	Subtype B Env					Subtype C Env					
	QH0692.42	TRO.11	pWITO 4160.33	pREJO 4541.67	SC4226 61.8	ZM214M .PL15	ZM249M PL1	ZM53M. PB12	ZM109F. PB4	ZM135M .PL10a	CAP210 .2.00.E8
R23		75	58	217				22			
R30							51			28	96
S7		44					84	53	177		
S23							44			296	
S31		142			49		131		180		
S34			44	35					86	95	

500 > ID50 > 100
100 > ID50 > 20
no neutralization

Figure 4. Anti-HIV-1 neutralizing activity of 6 selected plasma samples against B-Env- and C-Env-recombinant viruses. Neutralizing activity of 6 plasma samples against 5 B-Env- and 6 C-Env-recombinant viruses was evaluated as described in the legend to Figure 1. Data are presented as the means of at least three independent experiments. Plasma IDs and Env-recombinant viruses tested are denoted on the left side and above the panel, respectively. ID50 values 100–500 and 20–100 are highlighted in orange and yellow, respectively. No neutralization (ID50 values <20) of a recombinant virus is denoted by a gray background.
doi:10.1371/journal.pone.0053920.g004

Results

Neutralizing activity of plasma derived from rapid progressors

We evaluated the anti-HIV-1 neutralizing activity of plasma derived from 33 rapid progressors by measuring the inhibitory effect of plasma on a single round replication of previously established AE-Env-recombinant viruses [11,12]. The 8 AE-Env-recombinant viruses used in this study consisted of the recombinant viruses containing 2 dual-tropic AE-Env, 29CC1 and 41CC1, 2 CXCR4-tropic AE-Env, 98CC2 and 107CC2, and 4 CCR5-tropic AE-Env, 47CC11, 55PL1, 102CC2 and 105PL3 [12]. Plasma samples derived from 33 rapid progressors showed various levels of neutralizing activities against 8 AE-Env-recombinant viruses (Fig. 1). The replication of recombinant viruses containing AE-Env, 29CC1, 55PL1 and 107CC2, was inhibited by many plasma samples, whereas that of recombinant viruses, containing AE-Env, 47CC11 and 98CC2, was inhibited only by 3 and 4 plasma samples, respectively (Fig. 1). The inhibitory effect of plasma on the replication of 2 recombinant viruses containing dual-tropic AE-Env, 29CC1 and 41CC1, in U87.CD4.CCR5 was somewhat, but not significantly higher than that in U87.CD4.CXCR4 cells (data not shown), suggesting that viral entry through the CCR5 molecule is more susceptible to plasma-mediated neutralization than entry through CXCR4. Finally, plasma samples R23 and R30 inhibited the replication of most AE-Env-recombinant viruses tested, but failed to inhibit the replication of a recombinant virus containing AE-Env, 98CC2 (Fig. 1).

Neutralizing activity of plasma derived from slow progressors

We next evaluated the neutralizing activity of plasma derived from 34 slow progressors. The plasma samples showed various levels of neutralizing activity against AE-Env-recombinant viruses tested (Fig. 2). Plasma derived from slow progressors inhibited the replication of 8 AE-Env-recombinant viruses with a similar tendency to plasma derived from rapid progressors; however, the replication of 2 recombinant viruses containing AE-Env, 47CC11 and 98CC2 was inhibited more frequently by plasma derived from slow progressors than from rapid progressors (Figs. 1 and 2). In contrast, the replication of a recombinant virus containing AE-Env, 107CC2 was inhibited less frequently by plasma derived from slow progressors than from rapid progressors (Figs. 1 and 2). It is noteworthy that 4 plasma samples, S7, S23, S31 and S34, derived from slow progressors, inhibited the replication of all AE-Env-recombinant viruses tested, whereas no plasma from rapid progressors inhibited the replication of all recombinant viruses (Figs. 1 and 2).

Comparison of the breadth and potency of anti-HIV-1 neutralizing activity between the plasma derived from rapid and slow progressors

We next performed statistical analyses to compare the breadth and potency of neutralizing activity between the plasma derived from rapid and slow progressors. Viral neutralization was observed in 109 virus/plasma combinations among 264 virus/plasma combinations by the plasma derived from rapid progressors (Fig. 1), whereas it was observed in 101 virus/plasma combinations among 277 virus/plasma combinations by the plasma derived from slow progressors (Fig. 2). Fisher's exact test for a 2×2 contingency table revealed no statistical significance ($P>0.5$) in the breadth of viral neutralization between plasma derived from both groups. In addition, the mean ID50 values of plasma derived from rapid and slow progressors on viral neutralization were 227 and 200, respectively. Student's t-test revealed no statistical significance ($P>0.5$) in the potency of viral neutralization between plasma derived from both groups; therefore, we concluded that no clear differences were observed overall in the potency and breadth of anti-HIV-1 neutralizing activity in plasma derived from rapid and slow progressors. We next compared the proportion of AE-Env-recombinant viruses neutralized by a plasma sample and evaluated the neutralization breadth of plasma derived from rapid and slow progressors in more detail. The results showed that the replication of more than 60% (5 of 8) of AE-Env-recombinant viruses was inhibited by 24% (8 of 33) and 26% (9 of 34) of plasma derived from rapid and slow progressors, respectively (Fig. 3, bars above blue lines), suggesting no clear difference between the groups. In contrast, the replication of more than 80% (7 of 8) of AE-Env-recombinant viruses was inhibited by 21% (7 of 34) of plasma derived from slow progressors, whereas that was inhibited by 9% (3 of 33) of plasma derived from rapid progressors (Fig. 3, bars above red lines). These results showed that several plasma samples derived from slow progressors neutralized AE-Env-recombinant viruses more frequently than those from rapid progressors.

Plasma derived from Thai patients possessed CRF01_AE-specific neutralizing activity

We next studied the neutralizing activity of plasma, R23, R30, S7, S23, S31 and S34, which efficiently inhibited the replication of AE-Env-recombinant viruses, against 5 B-Env- and 6 C-Env-recombinant viruses. The results showed that these plasma samples were able to inhibit the replication of less than half of B-Env- and C-Env-recombinant viruses tested.

Discussion

In this report, we performed a comparative study on the anti-HIV-1 neutralizing activity of plasma samples derived from rapid and slow progressors residing in northern Thailand. Previous reports showed that broadly neutralizing activity against heterologous HIV-1 clinical isolates was more frequently detected in plasma or serum samples derived from long-term non-progressors (LTNP) than from progressors [19,20,21], suggesting the involvement of a broadly reactive neutralizing antibody response in regulating disease progression. In contrast, recent reports have shown that broadly neutralizing activity was more frequently detected in serum samples derived from slow and rapid progressors than from LTNP [22,23]. In addition, no correlation between the neutralization breadth of plasma and disease progression was observed in a recent longitudinal study of a seroincident cohort [24]; therefore, the role of the broadly neutralizing antibody response in HIV-1 disease control is unclear. Nevertheless, the anti-HIV-1 antibody response is a factor involved in regulating viral replication; therefore, it may be important to accumulate knowledge about how a strong humoral immune response is induced in some patients.

No statistically significant differences in the potency and breadth of neutralizing activities were observed overall in plasma derived from two groups of patients in this report (Figs. 1 and 2); however, several plasma samples derived from slow progressors were capable of neutralizing AE-Env-recombinant viruses more frequently than those from rapid progressors (Fig. 3), indicating the possible involvement of the anti-HIV-1 broadly reactive antibody response, at least in part, in controlling disease progression. In addition, broadly neutralizing human monoclonal antibodies, VRC01 and PG9, were recently established from

samples derived from a slow progressor and an elite neutralizer, respectively [7,8,25], indicating the possible correlation between the induction of potent and broadly neutralizing antibodies and slow disease progression. Broadly neutralizing antibodies are reported to be elicited in the early phase of HIV-1 infection [26]. In addition, such broadly reactive antibodies were elicited in an elite neutralizer within a year after viral infection [27]. Another report showed a correlation between viral load and the broadly neutralizing antibody response, as well as an inverse correlation between CD4 count and such an antibody response, in the early phase of HIV-1 infection [28]. Considering these reports, the induction mechanism of broadly neutralizing antibodies has been elucidated in part, but more information needs to be accumulated. The understanding of broadly neutralizing antibody responses induced by natural HIV-1 infection may provide valuable insights into the design of an effective HIV vaccine antigen using a reverse engineering approach. We studied the epitopes of anti-HIV-1 neutralizing antibodies in selected plasma samples that neutralized AE-Env-recombinant viruses efficiently; however, they were not revealed in this study. We consider that epitope analysis of broadly reactive plasma, as well as evaluation of the immunogenicity of Env gp120 and gp41 molecules derived from viruses isolated from patients with broadly neutralizing plasma, may be important in future studies.

The replication of B-Env- and C-Env-recombinant viruses was not efficiently inhibited by selected plasma that showed broadly neutralizing activity against AE-Env-recombinant viruses (Fig. 4). These results suggest that the antigenicity of Env gp120 and gp41 differs among CRF01_AE, subtype B and C viruses. Our results were consistent with the results described in a previous report that serum samples derived from subtype B and E (CRF01_AE) - infected Thai individuals showed subtype-specific neutralizing activity [29]. Env gp120 and gp41 are the most variable HIV-1 proteins, with typical intersubtype and intrasubtype differences reaching 35% and 20%, respectively [30]. In addition, structural differences between subtype B and C Env molecules have recently been reported [31]. Moreover, our recent observations suggested that different Env regions were affected by host immune pressure between CRF01_AE and subtype B viruses [32]. Taken together with the results in this report, we believe that it is important to take into account the antigenic and immunogenic diversity among different subtypes and CRFs of HIV-1 in developing HIV-1 vaccine antigens to elicit a broadly neutralizing antibody response.

Acknowledgments

We are grateful to Dr. Shigeyuki Hamada (RCC-ERI, Research Institute for Microbial Diseases, Osaka University) for his valuable help with this study. The manuscript was proofread by Medical English Service (Kyoto, Japan).

Author Contributions

Conceived and designed the experiments: N. Tsuchiya KA PI MK. Performed the experiments: SS. Analyzed the data: SS MK. Contributed reagents/materials/analysis tools: PP PS N. Takeda. Wrote the paper: SS MK.

References

1. Girard MP, Osmanov S, Assossou OM, Kieny MP (2011) Human immunodeficiency virus (HIV) immunopathogenesis and vaccine development: A review. Vaccine 29: 6191–6218.
2. Vaine M, Wang S, Liu Q, Arthos J, Montefiori D, et al. (2010) Profiles of human serum antibody responses elicited by three leading HIV vaccines focusing on the induction of Env-specific antibodies. PLoS ONE 5: e13916.
3. Barbas CF 3rd, Collet TA, Amberg W, Roben P, Binley JM, et al. (1993) Molecular profile of an antibody response to HIV-1 as probed by combinatorial libraries. J Mol Biol 230: 812–823.
4. Trkola A, Purtscher M, Muster T, Ballaun C, Buchacher A, et al. (1996) Human monoclonal antibody 2G12 defines a distinctive neutralization epitope on the gp120 glycoprotein of human immunodeficiency virus type 1. Journal of virology 70: 1100–1108.
5. Stiegler G, Kunert R, Purtscher M, Wolbank S, Voglauer R, et al. (2001) A potent cross-clade neutralizing human monoclonal antibody against a novel epitope on gp41 of human immunodeficiency virus type 1. AIDS research and human retroviruses 17: 1757–1765.
6. Purtscher M, Trkola A, Gruber G, Buchacher A, Predl R, et al. (1994) A broadly neutralizing human monoclonal antibody against gp41 of human immunodeficiency virus type 1. AIDS Research and Human Retroviruses 10: 1651–1658.
7. Walker LM, Phogat SK, Chan-Hui PY, Wagner D, Phung P, et al. (2009) Broad and potent neutralizing antibodies from an African donor reveal a new HIV-1 vaccine target. Science 326: 285–289.
8. Wu X, Yang ZY, Li Y, Hogerkorp CM, Schief WR, et al. (2010) Rational design of envelope identifies broadly neutralizing human monoclonal antibodies to HIV-1. Science 329: 856–861.
9. Hemelaar J, Gouws E, Ghys PD, Osmanov S (2011) Global trends in molecular epidemiology of HIV-1 during 2000-2007. AIDS 25: 679–689.
10. Arroyo MA, Phanuphak N, Krasaesub S, Sirivichayakul S, Assawadarachai V, et al. (2010) HIV type 1 molecular epidemiology among high-risk clients attending the Thai Red Cross Anonymous Clinic in Bangkok, Thailand. AIDS Res Hum Retroviruses 26: 5–12.
11. Utachee P, Jinnopat P, Isarangkura-Na-Ayuthaya P, de Silva UC, Nakamura S, et al. (2009) Phenotypic studies on recombinant human immunodeficiency virus type 1 (HIV-1) containing CRF01_AE env gene derived from HIV-1-infected patient, residing in central Thailand. Microbes Infect 11: 334–343.
12. Utachee P, Jinnopat P, Isarangkura-Na-Ayuthaya P, de Silva UC, Nakamura S, et al. (2009) Genotypic Characterization of CRF01_AE env Genes Derived from Human Immunodeficiency Virus Type 1-Infected Patients Residing in Central Thailand. AIDS Res Hum Retroviruses 25: 229–236.
13. Bjorndal A, Deng H, Jansson M, Fiore JR, Colognesi C, et al. (1997) Coreceptor usage of primary human immunodeficiency virus type 1 isolates varies according to biological phenotype. J Virol 71: 7478–7487.
14. Wei X, Decker JM, Liu H, Zhang Z, Arani RB, et al. (2002) Emergence of resistant human immunodeficiency virus type 1 in patients receiving fusion inhibitor (T-20) monotherapy. Antimicrob Agents Chemother 46: 1896–1905.
15. Li M, Gao F, Mascola JR, Stamatatos L, Polonis VR, et al. (2005) Human immunodeficiency virus type 1 env clones from acute and early subtype B infections for standardized assessments of vaccine-elicited neutralizing antibodies. J Virol 79: 10108–10125.
16. Wei X, Decker JM, Wang S, Hui H, Kappes JC, et al. (2003) Antibody neutralization and escape by HIV-1. Nature 422: 307–312.
17. Li M, Salazar-Gonzalez JF, Derdeyn CA, Morris L, Williamson C, et al. (2006) Genetic and neutralization properties of subtype C human immunodeficiency virus type 1 molecular env clones from acute and early heterosexually acquired infections in Southern Africa. J Virol 80: 11776–11790.
18. Kinomoto M, Yokoyama M, Sato H, Kojima A, Kurata T, et al. (2005) Amino acid 36 in the human immunodeficiency virus type 1 gp41 ectodomain controls fusogenic activity: implications for the molecular mechanism of viral escape from a fusion inhibitor. J Virol 79: 5996–6004.
19. Pilgrim AK, Pantaleo G, Cohen OJ, Fink LM, Zhou JY, et al. (1997) Neutralizing antibody responses to human immunodeficiency virus type 1 in primary infection and long-term-nonprogressive infection. The Journal of infectious diseases 176: 924–932.
20. Montefiori DC, Pantaleo G, Fink LM, Zhou JT, Zhou JY, et al. (1996) Neutralizing and infection-enhancing antibody responses to human immunodeficiency virus type 1 in long-term nonprogressors. The Journal of infectious diseases 173: 60–67.
21. Cao Y, Qin L, Zhang L, Safrit J, Ho DD (1995) Virologic and immunologic characterization of long-term survivors of human immunodeficiency virus type 1 infection. The New England journal of medicine 332: 201–208.
22. Doria-Rose NA, Klein RM, Daniels MG, O'Dell S, Nason M, et al. (2010) Breadth of human immunodeficiency virus-specific neutralizing activity in sera: clustering analysis and association with clinical variables. J Virol 84: 1631–1636.
23. Doria-Rose NA, Klein RM, Manion MM, O'Dell S, Phogat A, et al. (2009) Frequency and phenotype of human immunodeficiency virus envelope-specific B cells from patients with broadly cross-neutralizing antibodies. J Virol 83: 188–199.
24. Piantadosi A, Panteleeff D, Blish CA, Baeten JM, Jaoko W, et al. (2009) Breadth of neutralizing antibody response to human immunodeficiency virus type 1 is affected by factors early in infection but does not influence disease progression. J Virol 83: 10269–10274.
25. Simek MD, Rida W, Priddy FH, Pung P, Carrow E, et al. (2009) Human immunodeficiency virus type 1 elite neutralizers: individuals with broad and potent neutralizing activity identified by using a high-throughput neutralization assay together with an analytical selection algorithm. J Virol 83: 7337–7348.

26. Sather DN, Armann J, Ching LK, Mavrantoni A, Sellhorn G, et al. (2009) Factors associated with the development of cross-reactive neutralizing antibodies during human immunodeficiency virus type 1 infection. J Virol 83: 757–769.
27. Euler Z, van den Kerkhof TL, van Gils MJ, Burger JA, Edo-Matas D, et al. (2012) Longitudinal Analysis of Early HIV-1-Specific Neutralizing Activity in an Elite Neutralizer and in Five Patients Who Developed Cross-Reactive Neutralizing Activity. Journal of virology 86: 2045–2055.
28. Gray ES, Madiga MC, Hermanus T, Moore PL, Wibmer CK, et al. (2011) The Neutralization Breadth of HIV-1 Develops Incrementally over Four Years and Is Associated with CD4+ T Cell Decline and High Viral Load during Acute Infection. Journal of virology 85: 4828–4840.
29. Mascola JR, Louder MK, Surman SR, Vancott TC, Yu XF, et al. (1996) Human immunodeficiency virus type 1 neutralizing antibody serotyping using serum pools and an infectivity reduction assay. AIDS Research and Human Retroviruses 12: 1319–1328.
30. Gaschen B, Taylor J, Yusim K, Foley B, Gao F, et al. (2002) Diversity considerations in HIV-1 vaccine selection. Science 296: 2354–2360.
31. Gnanakaran S, Lang D, Daniels M, Bhattacharya T, Derdeyn CA, et al. (2007) Clade-specific differences between human immunodeficiency virus type 1 clades B and C: diversity and correlations in C3-V4 regions of gp120. J Virol 81: 4886–4891.
32. Boonchawalit S, Jullaksorn D, Uttiyoung J, Yowang A, Krathong N, et al. (2011) Molecular Evolution of HIV-1 CRF01_AE Env in Thai Patients. PLoS ONE 6: e27098.

Published May 29, 2013, doi:10.4049/jimmunol.1203217

IFN-γ–Producing Effector CD8 T Lymphocytes Cause Immune Glomerular Injury by Recognizing Antigen Presented as Immune Complex on Target Tissue

Ken Tsumiyama,* Akira Hashiramoto,† Mai Takimoto,† Sachiyo Tsuji-Kawahara,‡ Masaaki Miyazawa,‡ and Shunichi Shiozawa*

We investigated the role of effector CD8 T cells in the pathogenesis of immune glomerular injury. BALB/c mice are not prone to autoimmune disease, but after 12 immunizations with OVA they developed a variety of autoantibodies and glomerulonephritis accompanied by immune complex (IC) deposition. In these mice, IFN-γ–producing effector CD8 T cells were significantly increased concomitantly with glomerulonephritis. In contrast, after 12 immunizations with keyhole limpet hemocyanin, although autoantibodies appeared, IFN-γ–producing effector CD8 T cells did not develop, and glomerular injury was not induced. In β_2-microglobulin–deficient mice lacking CD8 T cells, glomerular injury was not induced after 12 immunizations with OVA, despite massive deposition of IC in the glomeruli. In mice containing a targeted disruption of the exon encoding the membrane-spanning region of the Ig μ-chain (μMT mice), 12 immunizations with OVA induced IFN-γ–producing effector CD8 T cells but not IC deposition or glomerular injury. When CD8 T cells from mice immunized 12 times with OVA were transferred into naive recipients, glomerular injury could be induced, but only when a single injection of OVA was also given simultaneously. Importantly, injection of OVA could be replaced by one injection of the sera from mice that had been fully immunized with OVA. This indicates that deposition of IC is required for effector CD8 T cells to cause immune tissue injury. Thus, in a mouse model of systemic lupus erythematosus, glomerular injury is caused by effector CD8 T cells that recognize Ag presented as IC on the target renal tissue. ***The Journal of Immunology*****, 2013, 191: 000–000.**

Glomerular injury is a major clinical feature of systemic lupus erythematosus (SLE) and is found in up to 50% of SLE patients. This injury has been attributed to the induction of an immunopathology resulting from immune complex (IC) deposition (1–7). However, it is also clear that IC by itself is not sufficient for the development of glomerular injury (8–11) and that CD4 T cells also contribute to the glomerular injury seen in SLE. Wofsy et al. (12–14) and Jabs et al. (15) showed that anti-CD4 T cell Ab therapy could significantly reduce the frequency and the extent of glomerulonephritis in both NZB/W F_1 and MRL/*lpr* mouse models of lupus. Jevnikar et al. (16) showed that deficiency of MHC class II results in the amelioration of autoimmune renal disease in MRL/*lpr* mice. In contrast, Chesnutt et al. (17) showed that nephritis is not abolished in CD4-deficient MRL/*lpr* mice, whereas Christianson et al. (18) and Chan et al. (19) showed that glomerular injury is prevented in MHC class I–deficient MRL/*lpr* mice, which lack CD8 T cells. D'Agati et al. (20) showed that CD8, rather than CD4, T cells predominate in most of the biopsied kidney samples from patients with SLE. Couzi et al. (21) showed that CD8 T cells predominantly infiltrate to the periglomerular region of lupus kidney and are significantly associated with the prognosis of lupus nephritis. Together, these findings reinforce the importance of CD8 T cells in the pathogenesis of lupus nephritis. Nevertheless, discrepancies still exist in assessing the contribution of CD4 versus CD8 T cells to glomerular injury and IC deposition (22–25). Thus, we wished to better clarify the role of CD8 T cells in this pathology.

We previously succeeded in inducing glomerular injury with characteristics almost identical to human SLE in mice normally not prone to autoimmune disease (26). In that study, we showed that both CD4 T cell help and Ag cross-presentation are fundamental for activating CD8 T cells to become fully matured CTLs and, subsequently, to induce lupus kidney disease. If this finding is correct, then discrepancies in the literature describing differing contributions of CD4 or CD8 T cells to lupus nephritis (12–21) might be reconciled. Therefore, in the current study, we used β_2-microglobulin (β_2m)-deficient mice, which lack functional effector CTLs, and mice harboring a targeted disruption of the exon encoding the membrane-spanning region of the Ig μ-chain (μMT), which lack B cells, to examine the relationships among IC deposition, effector CD8 T cells, and the nephritis induced in mice by repeated immunization with OVA.

Materials and Methods

Animal studies

Animal studies were performed with the approval of the Institutional Animal Care And Use Committee and according to animal experimental regulations at Kobe University and Kyushu University. Eight-week-old

*Department of Medicine, Kyushu University Beppu Hospital, Beppu 874-0838, Japan; †Department of Biophysics, Kobe University Graduate School of Health Science, Kobe 654-0142, Japan; and ‡Department of Immunology, Kinki University School of Medicine, Osaka-Sayama 589-8511, Japan

Received for publication November 21, 2012. Accepted for publication May 1, 2013.

This work was supported by a Global Center of Excellence Program Grant from the Ministry of Education, Culture, Sports, Science and Technology of Japan, as well as the Japan Science and Technology Organization (to S.S.). S.S. is an investigator of the Global Center of Excellence, Japan.

Address correspondence and reprint requests to Prof. Shunichi Shiozawa, Department of Medicine, Kyushu University Beppu Hospital, 4546 Tsurumihara, Tsurumi, Beppu 874-0838, Japan. E-mail address: shiozawa@beppu.kyushu-u.ac.jp

Abbreviations used in this article: AU, arbitrary unit; IC, immune complex; KLH, keyhole limpet hemocyanin; β_2m, β_2-microglobulin; μMT, targeted disruption of the exon encoding the membrane-spanning region of the Ig μ-chain; RF, rheumatoid factor; SLE, systemic lupus erythematosus; Treg, regulatory T cell; WT, wild-type.

female BALB/c mice (Japan SLC, Hamamatsu, Japan), β_2m-deficient mice (BALB/c background) (27), and μMT mice (BALB/c background) (28) were immunized with 500 μg OVA (grade V; Sigma, St. Louis, MO), 100 μg keyhole limpet hemocyanin (KLH; Sigma), or PBS by i.p. injection every 5 d. Nine days after the final immunization, proteinuria was measured semiquantitatively using urine dipsticks (Albstix; Siemens Healthcare Diagnostics, Tarrytown, NY), and B, T, CD4 T, and CD8 T cells were isolated from spleen to >90% purity using MACS beads (Miltenyi Biotec, Bergisch Gladbach, Germany). Isolated cells were adoptively transferred i.v. into naive BALB/c mice (2.5×10^7/mouse), and an additional booster i.p. injection of 500 μg OVA or 500 μl sera from mice immunized 12 times with OVA was given at 24 h after transfer. Sera, urine, and organs were collected 2 wk later. CD4 and CD8 T cells in the kidney were analyzed by flow cytometry 9 d after the final immunization with allophycocyanin-conjugated anti-CD4 Abs (RM4-5; BioLegend, San Diego, CA) and PerCP-conjugated anti-CD8 Abs (53-6.7; BD Pharmingen, San Diego, CA). Glomerular injury in mice was evaluated by studying 30 glomeruli/mouse.

Immunofluorescent staining

Frozen kidney sections were stained for C3 and IgG using goat anti-C3 Abs (Bethyl Laboratories, Montgomery, TX), Alexa Fluor 488–conjugated anti-goat IgG Abs, or Alexa Fluor 594–conjugated anti-mouse IgG Abs (both from Molecular Probes, Eugene, OR).

Intracellular IFN-γ staining

Spleen cells (1×10^6/ml) were stimulated with 50 ng/ml PMA and 500 ng/ml ionomycin in the presence of brefeldin A (10 μg/ml; all from Sigma) for 4 h and stained with PerCP-conjugated anti-CD8 Ab, followed by fixation in 2% formaldehyde, permeabilization with 0.5% saponin (Sigma), and staining with PE-conjugated anti–IFN-γ Ab (XMG1.2; BD Pharmingen).

ELISA

Sera were assayed for rheumatoid factor (RF) by ELISA (Shibayagi, Gunma, Japan), for anti-Sm Ab using plates coated with Sm Ag (ImmunoVision, Springdale, AR), and for anti-dsDNA Ab using plates coated with dsDNA (Worthington Biochemical, Lakewood, NJ) that had been digested using S1 nuclease (Promega, Madison, WI). Serum IgG, IgG1, and IgG2a were measured by ELISA (Bethyl Laboratories). Serum IC was measured using anti-C3 Ab (Bethyl Laboratories) and HRP-conjugated anti-mouse IgG Ab (Kirkegaard & Perry Laboratories, Gaithersburg, MD), followed by reaction with *o*-phenylenediamine (Sigma). An arbitrary unit (AU) of 1.0 is the equivalent of the titer found in sera of 25-wk-old MRL/*lpr* mice. Anti-OVA Ab in sera was quantified as a reference using mouse anti-OVA mAb (OVA-14; Sigma).

Statistical analysis

Statistical analyses were performed using the Student *t* test, and the data are expressed as the mean ± SD.

Results

Requirement of activated CD8 T cells for glomerular injury

Wild-type (WT) BALB/c mice, which are normally not prone to autoimmune disease, were repeatedly immunized with OVA every 5 d. After 12 immunizations, we observed an increase in autoantibodies, including RF, anti-Sm, and anti-dsDNA Abs, and an increase in serum IC and glomerular injury (Fig. 1A, 1B). Glomerular injury was assessed by proteinuria and glomerulonephritis, according to the International Society of Nephrology/Renal Pathology Society classification. Glomerular injury consisted of the following: class II mesangial proliferative glomerulonephritis in 26.29 ± 7.53% of the specimens (n = 9, mean ± SD) (Fig. 1Ca), class III focal glomerulonephritis in 13.70 ± 7.53% of the specimens (Fig. 1Cb), class IV diffuse glomerulonephritis in 38.14 ± 7.28% of the specimens (Fig. 1Cc), class V membranous glomerulonephritis in 3.70 ± 3.51% of the specimens (Fig. 1Cd), and class VI advanced sclerosing glomerulonephritis in 10.37 ± 3.09% of the glomerular specimens (n = 9, mean ± SD) (Fig. 1Ce). We also immunized mice 12 times with KLH and observed a similar induction of RF and anti-Sm Ab; however, there was no anti-dsDNA Ab induction, proteinuria, or glomerular injury (Fig. 1A, 1B). We also observed an increase in serum IC and the massive deposition of IC in the glomeruli of mice. Serum IgG1 and IgG2a, which were reported to increase concomitantly with autoimmune renal diseases (29, 30), were also increased after immunization with either OVA or KLH (Fig. 1D). Importantly, however, we noted that IFN-γ–producing activated CD8 T cells were increased in OVA-immunized, but not KLH-immunized, mice (Fig. 1E). These IFN-γ–producing CD8 T cells infiltrated into the sites of OVA deposition in the glomeruli of the mice immunized 12 times with OVA (26). Compared with KLH-immunized and control mice, there were increased numbers of CD8 T cells, but not CD4 T cells, in the kidneys of OVA-immunized mice (Fig. 1F). This indicates that mice immunized 12 times with KLH do not induce effector CD8 T cells, which suggests that, despite the massive deposition of IC in the kidneys, the lack of glomerular injury in these mice is due to the fact that KLH was not cross-presented to T cells.

Glomerular injury induced by repeated OVA immunization could be adoptively transferred into naive recipients via $CD8^+$ T cell transfer (Fig. 2A). This adoptive transfer of glomerular injury was not accompanied by the generation of autoantibodies (26) or by any significant increase in IC or anti-OVA Ab in sera of the recipient mice (Fig. 2B). IC was only minimally deposited in the glomeruli of recipients, because they were boosted only once with OVA after cell transfer. Thus, these findings suggest that CD8 T cells are required for the generation of glomerular injury, whereas massive IC deposition is not required, although low amounts of IC deposition may still be necessary.

To prove that effector CD8 T cells are required for immune glomerular injury, we immunized β_2m-deficient mice, which lack functional effector CTLs (27). Following 12 immunizations of these mice with OVA, there was a marked increase in serum autoantibodies, including anti-dsDNA Ab (26), IC, and anti-OVA Ab, and there was massive deposition of IC in the kidney (Fig. 3B, 3C). However, glomerular injury was minimal, as demonstrated by low proteinuria (Fig. 3A) and the absence of glomerulonephritis by histopathologic analysis (Fig. 3B). This finding indicates that functional effector CD8 T cells are required for the induction of immune glomerular injury.

Requirement of IC

We next tested whether the presence of Ag in the form of IC is required for immune glomerular injury. For this, we used μMT mice, which lack B cells, do not induce Ag-specific Ab responses (28), and do not generate detectable IC in sera even after 12 immunizations with OVA (data not shown). In these mice, IC deposition and renal disease were both absent (Fig. 4A, 4B). However, IFN-γ–producing CD8 T cells developed to levels comparable to those seen in WT mice (Fig. 4C). This indicates that deposition of Ag in the form of IC is required before effector CD8 T cells can cause glomerular injury. To verify this further, we performed serum-transfer experiments. When CD8 T cells from mice immunized 12 times with OVA were transferred into naive recipients, they could reproducibly induce glomerular injury, but only when a single injection of OVA was given simultaneously (Fig. 2A). We subsequently tested whether one injection of sera from mice immunized 12 times with OVA could substitute for the single booster injection of OVA. We found that IC was indeed deposited in the recipients' glomeruli and was accompanied by glomerular injury at 2 wk after the transfer of CD8 T cells (Fig. 5). This demonstrates that deposition of at least some amount of Ag

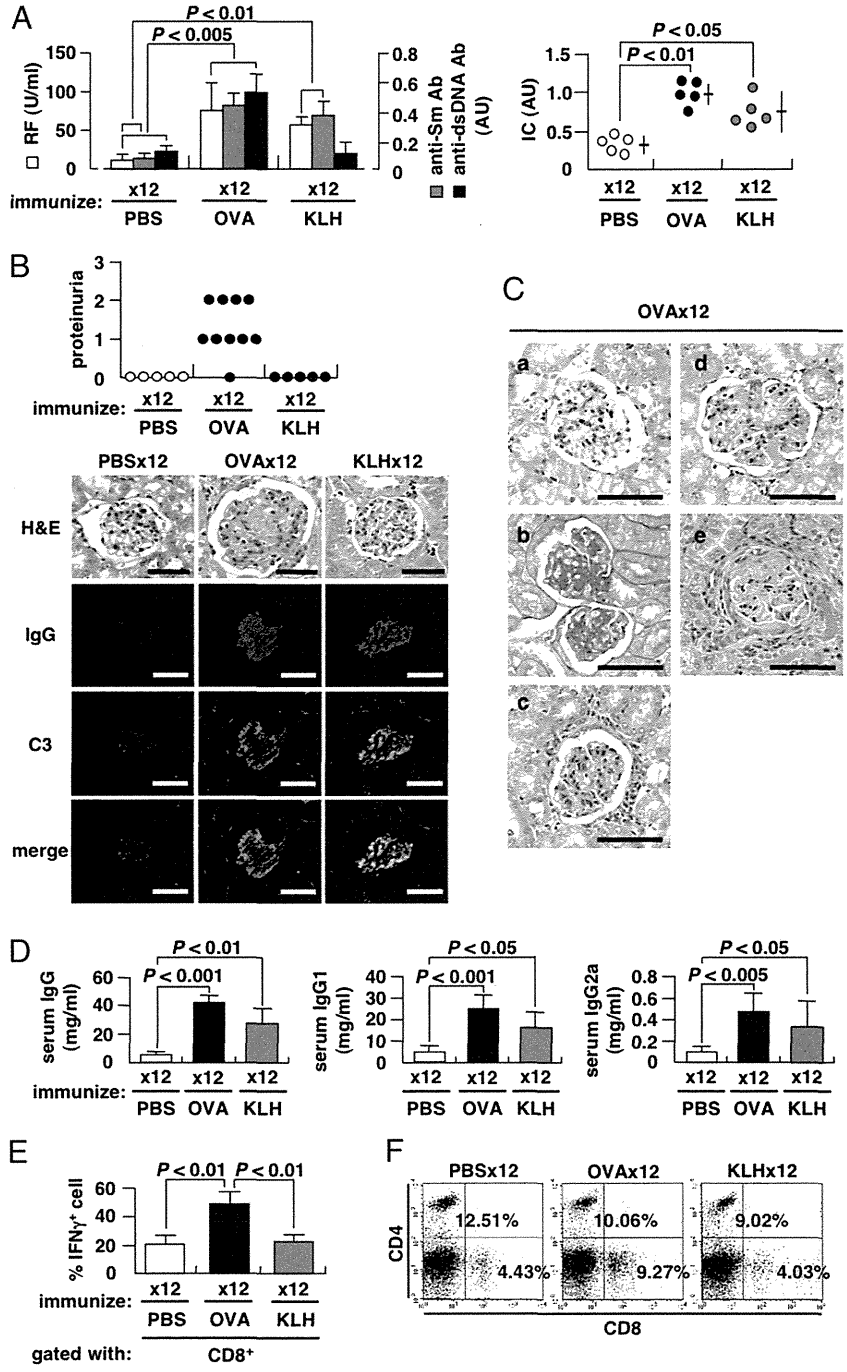

FIGURE 1. Renal disease is induced by repeated immunization with OVA but not with KLH. BALB/c mice were repeatedly injected i.p. with 500 μg of OVA, 100 μg of KLH, or PBS every 5 d. (**A**) Serum RF, anti-Sm, and anti-dsDNA Abs (*left panel*) and IC (*right panel*) were quantified by ELISA 2 d after final immunization (mean ± SD; 5 mice/group). AU refers to the value obtained with the sera of MRL/*lpr* mice. (**B**) Proteinuria was assessed 9 d after the final immunization and graded with a score of 0 (<30 mg/dl); 1 (30–99 mg/dl); 2 (100–299 mg/dl); or 3 (300–999 mg/dl). Kidney histopathology (H&E; scale bar, 50 μm; original magnification ×400; *top row*) and deposition of IC, IgG, and C3 in the glomeruli of the mice immunized 12 times with PBS, OVA, or KLH (scale bar, 50 μm; original magnification ×300; *second, third,* and *fourth rows*). (**C**) Representative kidney histopathology stained with H&E or periodic acid-Schiff and classified according to the International Society of Nephrology/Renal Pathology Society (scale bar, 50 μm; original magnification ×400). (**a**) Class II mesangial proliferative glomerulonephritis. (**b**) Class III focal glomerulonephritis. (**c**) Class IV diffuse glomerulonephritis. (**d**) Class V membranous glomerulonephritis. (**e**) Class VI advanced sclerosing glomerulonephritis. (**D**) Serum IgG, IgG1, and IgG2a assayed by ELISA 2 d after final immunization (mean ± SD, 5 mice/group). (**E**) Spleen cells stimulated with 50 ng/ml of PMA and 500 ng/ml of ionomycin for 4 h in the presence of brefeldin A (10 μg/ml) and stained for intracellular IFN-γ (mean ± SD, 5 mice/group). (**F**) Infiltrating CD4 and CD8 T cells from the kidneys of mice immunized 12 times with OVA or KLH were extracted and detected by flow cytometry. Each experiment was performed three times independently.

in the form of IC is required for effector CD8 T cells to exert their cytotoxicity and induce immune glomerular injury.

Discussion

The results in this study show that IFN-γ–producing effector CD8 T cells, which can recognize Ag presented as IC on target tissue, are required for the induction of glomerular injury in this mouse model of SLE. This finding is consistent with results showing that CD8 T cells are the dominant T cell population in renal biopsy specimens from lupus patients who presented with class III and IV glomerulonephritis (21). Heymann et al. (11) showed that glomerular Ag-specific CTLs induce renal immunopathology with the help of CD4 T cells. Such cooperation between CD8 and CD4 cells is indeed likely and may also explain several somewhat contradictory reports describing the contributions of CD8 and/or CD4 T cells to the pathogenesis of immune glomerular disease (12–21). In a previous study of experimentally induced SLE, we found that both Ag cross-presentation and CD4 T cell help were essential for generating effector CD8 CTLs, leading to glomerular injury (26). We proposed the "self-organized criticality theory," which explains that systemic autoimmunity, or SLE, necessarily takes place when a host's immune system is overstimulated by repeated exposure to Ag, achieving levels that surpass the immune system's stability limit (i.e., self-organized criticality). This theory proposes that autoreactive lymphocyte clones are newly generated via de novo TCR revision from nonautoreactive clones at the periphery (26, 31). We named this novel T cell type an autoantibody-inducing CD4 T cell and postulated that these cells stimulate B cells to generate various autoantibodies, as well as to promote the final differentiation of CD8 T cells into CTLs via Ag cross-

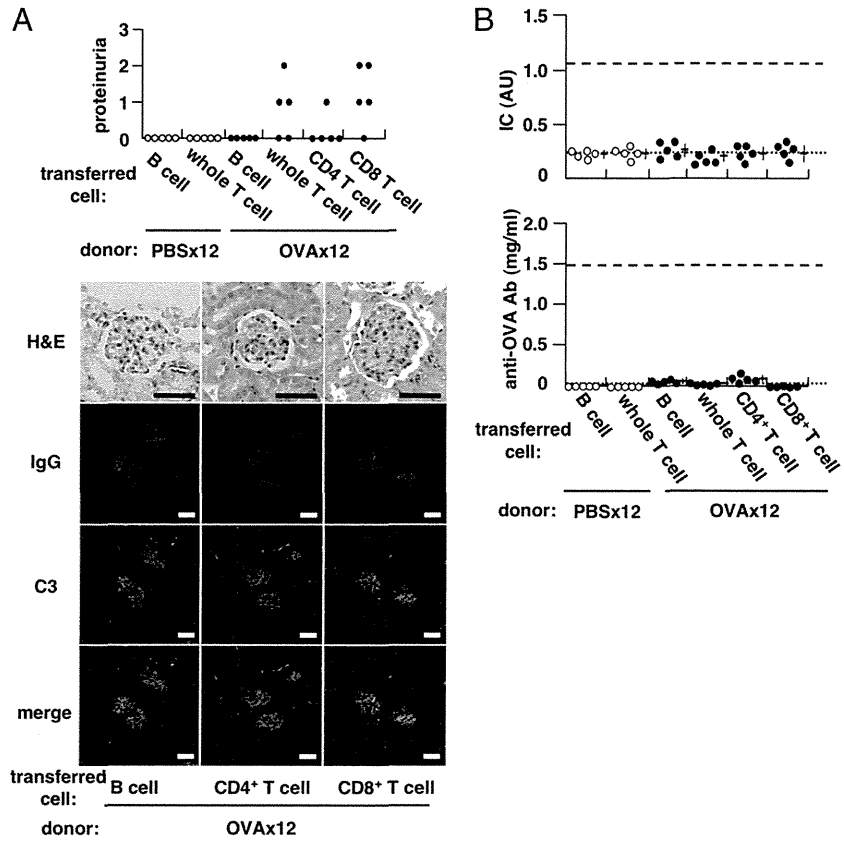

FIGURE 2. Glomerular injury is transferrable via fully matured effector CD8 T cells. Splenocytes of OVA-immunized BALB/c mice were adoptively transferred to naive recipients, and the recipients were injected with 500 μg of OVA 24 h after transfer. (**A**) Proteinuria, histopathology (H&E; scale bar, 50 μm; original magnification ×400) and the deposition of IC, IgG, and C3 in the glomeruli of recipient mice (scale bar, 50 μm; original magnification ×200) 2 wk after cell transfer. (**B**) Serum IC and anti-OVA Ab in recipients as measured by ELISA 2 wk after cell transfer (mean ± SD). Thin or bold dotted lines represent the averaged value in the donor mice immunized 12 times with PBS or OVA, respectively. AU refers to the value obtained with sera of MRL/*lpr* mice. Each experiment was performed twice independently.

presentation, leading to the tissue injuries found in SLE. Such a scenario is consistent with the previously demonstrated roles of CD8 and/or CD4 T cells in the pathogenesis of kidney disease (12–21) (i.e., CD8 T cells must mature into effector CD8 T cells with the help of CD4 T cells, primarily in the induction phase of glomerulonephritis).

In the current study, with regard to the role of effector CD8 T cells in the effector phase of glomerulonephritis, we focused on whether effector CD8 cells were directly responsible for the induction of glomerular injury. First, we found that effector CD8 T cells recognized Ag presented as IC on target renal tissue and consequently exerted immune glomerular injury. Glomerulone-

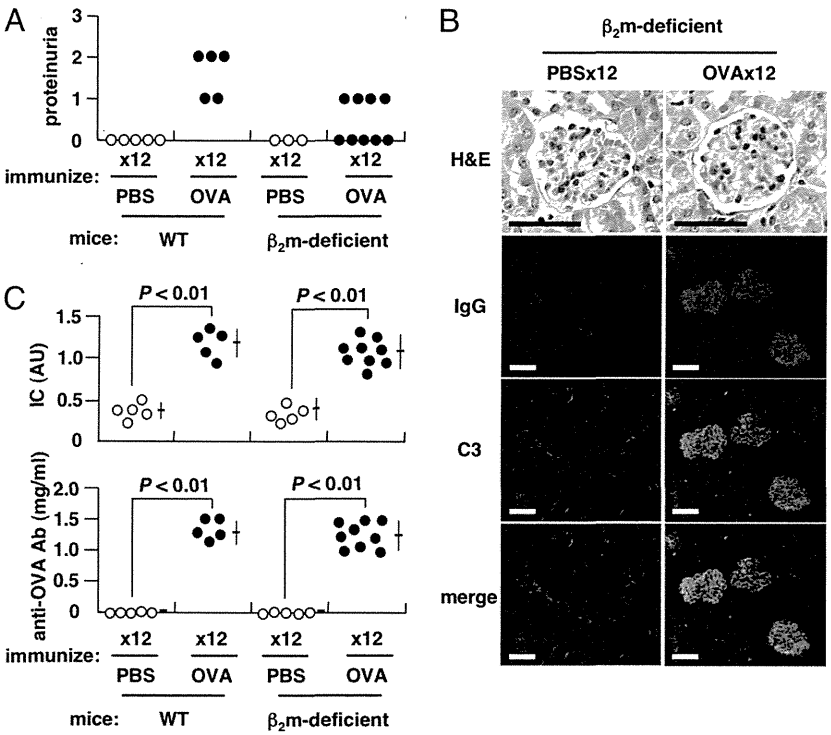

FIGURE 3. Glomerular injury is minimal in β_2m-deficient mice. β_2m-deficient mice were repeatedly injected i.p. with 500 μg OVA or PBS every 5 d. (**A**) Proteinuria in WT or β_2m-deficient mice assayed 9 d after 12 immunizations with OVA. (**B**) Histopathology (H&E; scale bar, 50 μm; original magnification ×400) and the deposition of IC, IgG, and C3 in the glomeruli of β_2m-deficient mice immunized 12 times with PBS or OVA (scale bar, 50 μm; original magnification ×200). (**C**) Serum IC and anti-OVA Ab measured by ELISA 2 d after 12 immunizations with OVA (mean ± SD). AU refers to value obtained with sera of MRL/*lpr* mice. Each experiment was performed three times independently.

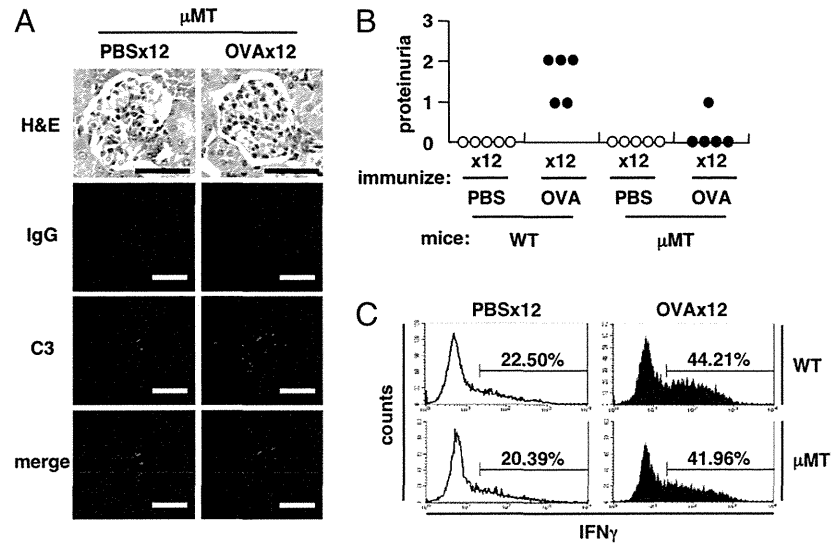

FIGURE 4. IC deposition and effector CD8 T cell–induced glomerular injury. μMT mice were repeatedly injected i.p. with 500 μg OVA or PBS every 5 d. (**A**) Histopathology (scale bar, 50 μm; original magnification ×400) and the deposition of IC, IgG, and C3 in the glomeruli of μMT mice immunized 12 times with PBS or OVA (scale bar, 50 μm; original magnification ×300). (**B**) Proteinuria in WT or μMT mice assayed 9 d after 12 immunizations with OVA. (**C**) IFN-γ–producing CD8 T cells in spleen of μMT mice immunized 12 times with OVA. Each experiment was performed three times independently.

phritis was not observed in the absence of effector CD8 T cells. Second, there must be at least some minimal amount of IC deposited on the target renal tissues for effector CD8 T cells to cause immune injury.

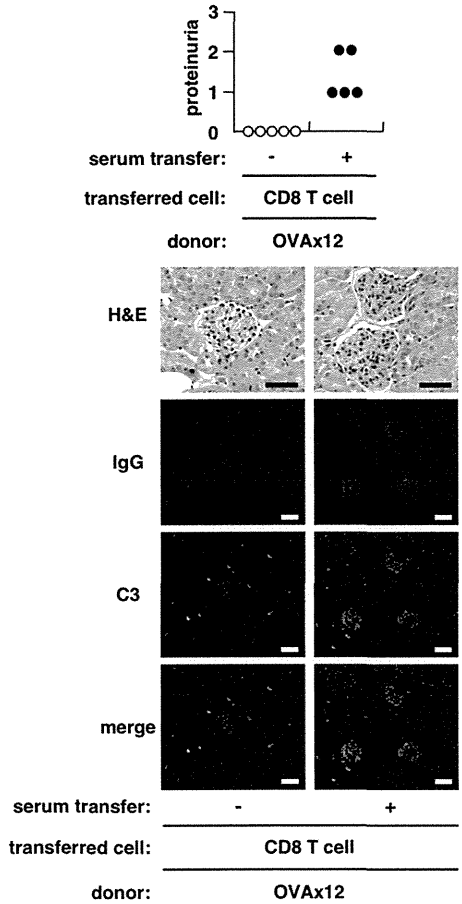

FIGURE 5. Requirement of IC deposition for effector CD8 T cell and subsequent glomerular injury. CD8 T cells from OVA-immunized BALB/c mice were adoptively transferred to naive recipients. The recipients were also injected once with 500 μl of sera from mice immunized 12 times with OVA 24 h after cell transfer. Shown are proteinuria, histopathology (H&E, scale bar, 50 μm; original magnification ×400), and the deposition of IC, IgG, and C3 in the glomeruli of recipient mice (scale bar, 50 μm; original magnification ×200) 2 wk after cell transfer.

Previous studies showed that β_2m is required for the surface expression of MHC class I, as well as CD1d and Qa-1. Although lack of CD1d expression can lead to NKT cell deficiency (32), we found that repeated OVA immunization of CD1d knockout mice led to both the production of various autoantibodies and the development of proteinuria to the same degree observed in WT mice (K. Tsumiyama and S. Shiozawa, manuscript in preparation). Qa-1 plays important roles in the suppression of CD4 T cells and CD8 regulatory T cell (Treg) functions (33, 34). Deficiency of Qa-1 causes exaggerated secondary CD4 responses against virus or self-peptide and impairs CD8 Treg function, ultimately leading to autoimmunity (35, 36). However, we found that the levels of autoantibodies generated after 12 repeated immunizations with OVA were similar between β_2m-deficient mice and WT mice (Supplemental Fig. 3 in Ref. 26). In addition, tissue injuries, including glomerulonephritis, were clearly not induced in the β_2m-deficient mice (Fig. 3), even in mice that had received CD8 T cells transferred from OVA-stimulated WT mice (figure 1C of in Ref. 26). In previous studies, the phenotype of inhibitory CD8 Tregs was shown to fluctuate (37–40). Inhibitory CD8 Treg function was reported to be defective in human SLE patients and in animal models of SLE (41–43). However, it was also observed that lupus nephritis can be suppressed by anti-CD8 Ab treatment or by MHC class I deficiency (18, 19, 44). Further, recent studies show that Tregs are actually required for the final differentiation of CD8 T cells (45). Thus, CD1d, Qa-1, NKT cells, or CD8 Tregs do not appear to play a causative role in immune-mediated glomerular disease.

In summary, immune tissue injury requires, first, that CD8 T cells mature into effector cells with the help of CD4 T cells, primarily in the induction phase. Second, in the effector phase, effector CD8 T cells recognize Ag presented as IC on target tissue, and this recognition is required for their cytotoxic actions.

Acknowledgments

We thank Dr. Norishige Yoshikawa (Wakayama Medical University, Wakayama, Japan) and Dr. Marc Lamphier (Eisai Co. Ltd., Tokyo, Japan) for useful advice and critical review of the manuscript.

Disclosures

The authors have no financial conflicts of interest.

References

1. Tan, E. M., P. H. Schur, R. I. Carr, and H. G. Kunkel. 1966. Deoxybonucleic acid (DNA) and antibodies to DNA in the serum of patients with systemic lupus erythematosus. *J. Clin. Invest.* 45: 1732–1740.
2. Koffler, D., P. H. Schur, and H. G. Kunkel. 1967. Immunological studies concerning the nephritis of systemic lupus erythematosus. *J. Exp. Med.* 126: 607–624.
3. Dixon, F. J., M. B. Oldstone, and G. Tonietti. 1971. Pathogenesis of immune complex glomerulonephritis of new zealand mice. *J. Exp. Med.* 134: 65–71.
4. Pankewycz, O. G., P. Migliorini, and M. P. Madaio. 1987. Polyreactive autoantibodies are nephritogenic in murine lupus nephritis. *J. Immunol.* 139: 3287–3294.
5. Vlahakos, D. V., M. H. Foster, S. Adams, M. Katz, A. A. Ucci, K. J. Barrett, S. K. Datta, and M. P. Madaio. 1992. Anti-DNA antibodies form immune deposits at distinct glomerular and vascular sites. *Kidney Int.* 41: 1690–1700.
6. Shlomchik, M. J., M. P. Madaio, D. Ni, M. Trounstein, and D. Huszar. 1994. The role of B cells in *lpr/lpr*-induced autoimmunity. *J. Exp. Med.* 180: 1295–1306.
7. Chan, O. T., M. P. Madaio, and M. J. Shlomchik. 1999. B cells are required for lupus nephritis in the polygenic, Fas-intact MRL model of systemic autoimmunity. *J. Immunol.* 163: 3592–3596.
8. Clynes, R., C. Dumitru, and J. V. Ravetch. 1998. Uncoupling of immune complex formation and kidney damage in autoimmune glomerulonephritis. *Science* 279: 1052–1054.
9. Schiffer, L., J. Sinha, X. Wang, W. Huang, G. von Gersdorff, M. Schiffer, M. P. Madaio, and A. Davidson. 2003. Short term administration of costimulatory blockade and cyclophosphamide induces remission of systemic lupus erythematosus nephritis in NZB/W F_1 mice by a mechanism downstream of renal immune complex deposition. [Published erratum appears in 2003 *J. Immunol.* 171: 1610.] *J. Immunol.* 171: 489–497.
10. Bagavant, H., U. S. Deshmukh, H. Wang, T. Ly, and S. M. Fu. 2006. Role for nephritogenic T cells in lupus glomerulonephritis: progression to renal failure is accompanied by T cell activation and expansion in regional lymph nodes. *J. Immunol.* 177: 8258–8265.
11. Heymann, F., C. Meyer-Schwesinger, E. E. Hamilton-Williams, L. Hammerich, U. Panzer, S. Kaden, S. E. Quaggin, J. Floege, H. J. Gröne, and C. Kurts. 2009. Kidney dendritic cell activation is required for progression of renal disease in a mouse model of glomerular injury. *J. Clin. Invest.* 119: 1286–1297.
12. Wofsy, D., and W. E. Seaman. 1985. Successful treatment of autoimmunity in NZB/NZW F_1 mice with monoclonal antibody to L3T4. *J. Exp. Med.* 161: 378–391.
13. Wofsy, D., and W. E. Seaman. 1987. Reversal of advanced murine lupus in NZB/NZW F_1 mice by treatment with monoclonal antibody to L3T4. *J. Immunol.* 138: 3247–3253.
14. Connolly, K., J. R. Roubinian, and D. Wofsy. 1992. Development of murine lupus in CD4-depleted NZB/NZW mice. Sustained inhibition of residual CD4+ T cells is required to suppress autoimmunity. *J. Immunol.* 149: 3083–3088.
15. Jabs, D. A., C. L. Burek, Q. Hu, R. C. Kuppers, B. Lee, and R. A. Prendergast. 1992. Anti-CD4 monoclonal antibody therapy suppresses autoimmune disease in MRL/Mp-lpr/lpr mice. *Cell. Immunol.* 141: 496–507.
16. Jevnikar, A. M., M. J. Grusby, and L. H. Glimcher. 1994. Prevention of nephritis in major histocompatibility complex class II-deficient MRL-*lpr* mice. *J. Exp. Med.* 179: 1137–1143.
17. Chesnutt, M. S., B. K. Finck, N. Killeen, M. K. Connolly, H. Goodman, and D. Wofsy. 1998. Enhanced lymphoproliferation and diminished autoimmunity in CD4-deficient MRL/*lpr* mice. *Clin. Immunol. Immunopathol.* 87: 23–32.
18. Christianson, G. J., R. L. Blankenburg, T. M. Duffy, D. Panka, J. B. Roths, A. Marshak-Rothstein, and D. C. Roopenian. 1996. β_2-microglobulin dependence of the lupus-like autoimmune syndrome of MRL-*lpr* mice. *J. Immunol.* 156: 4932–4939.
19. Chan, O. T., V. Paliwal, J. M. McNiff, S. H. Park, A. Bendelac, and M. J. Shlomchik. 2001. Deficiency in β(2)-microglobulin, but not CD1, accelerates spontaneous lupus skin disease while inhibiting nephritis in MRL-Fas(lpr) nice: an example of disease regulation at the organ level. *J. Immunol.* 167: 2985–2990.
20. D'Agati, V. D., G. B. Appel, D. Estes, D. M. Knowles, II, and C. L. Pirani. 1986. Monoclonal antibody identification of infiltrating mononuclear leukocytes in lupus nephritis. *Kidney Int.* 30: 573–581.
21. Couzi, L., P. Merville, C. Deminière, J. F. Moreau, C. Combe, J. L. Pellegrin, J. F. Viallard, and P. Blanco. 2007. Predominance of CD8+ T lymphocytes among periglomerular infiltrating cells and link to the prognosis of class III and class IV lupus nephritis. *Arthritis Rheum.* 56: 2362–2370.
22. Tipping, P. G., and S. R. Holdsworth. 2006. T cells in crescentic glomerulonephritis. *J. Am. Soc. Nephrol.* 17: 1253–1263.
23. Foster, M. H. 2007. T cells and B cells in lupus nephritis. *Semin. Nephrol.* 27: 47–58.
24. Bagavant, H., and S. M. Fu. 2009. Pathogenesis of kidney disease in systemic lupus erythematosus. *Curr. Opin. Rheumatol.* 21: 489–494.
25. Nowling, T. K., and G. S. Gilkeson. 2011. Mechanisms of tissue injury in lupus nephritis. *Arthritis Res. Ther.* 13: 250.
26. Tsumiyama, K., Y. Miyazaki, and S. Shiozawa. 2009. Self-organized criticality theory of autoimmunity. *PLoS ONE* 4: e8382.
27. Koller, B. H., P. Marrack, J. W. Kappler, and O. Smithies. 1990. Normal development of mice deficient in beta 2M, MHC class I proteins, and CD8+ T cells. *Science* 248: 1227–1230.
28. Kitamura, D., J. Roes, R. Kühn, and K. Rajewsky. 1991. A B cell-deficient mouse by targeted disruption of the membrane exon of the immunoglobulin mu chain gene. *Nature* 350: 423–426.
29. Richards, H. B., M. Satoh, J. C. Jennette, B. P. Croker, H. Yoshida, and W. H. Reeves. 2001. Interferon-γ is required for lupus nephritis in mice treated with the hydrocarbon oil pristane. *Kidney Int.* 60: 2173–2180.
30. Pérez de Lema, G., H. Maier, T. J. Franz, M. Escribese, S. Chilla, S. Segerer, N. Camarasa, H. Schmid, B. Banas, S. Kalaydjiev, et al. 2005. Chemokine receptor Ccr2 deficiency reduces renal disease and prolongs survival in MRL/lpr lupus-prone mice. *J. Am. Soc. Nephrol.* 16: 3592–3601.
31. Shiozawa, S. 2012. Pathogenesis of SLE and *ai*CD4T cell: new insight on autoimmunity. *Joint Bone Spine* 79: 428–430.
32. Smiley, S. T., M. H. Kaplan, and M. J. Grusby. 1997. Immunoglobulin E production in the absence of interleukin-4-secreting CD1-dependent cells. *Science* 275: 977–979.
33. Lu, L., M. B. Werneck, and H. Cantor. 2006. The immunoregulatory effects of Qa-1. *Immunol. Rev.* 212: 51–59.
34. Kim, H. J., and H. Cantor. 2011. Regulation of self-tolerance by Qa-1-restricted CD8(+) regulatory T cells. *Semin. Immunol.* 23: 446–452.
35. Hu, D., K. Ikizawa, L. Lu, M. E. Sanchirico, M. L. Shinohara, and H. Cantor. 2004. Analysis of regulatory CD8 T cells in Qa-1-deficient mice. *Nat. Immunol.* 5: 516–523.
36. Kim, H. J., B. Verbinnen, X. Tang, L. Lu, and H. Cantor. 2010. Inhibition of follicular T-helper cells by CD8(+) regulatory T cells is essential for self tolerance. *Nature* 467: 328–332.
37. Zheng, S. G., J. H. Wang, M. N. Koss, F. Quismorio, Jr., J. D. Gray, and D. A. Horwitz. 2004. $CD4^+$ and $CD8^+$ regulatory T cells generated ex vivo with IL-2 and TGF-β suppress a stimulatory graft-versus-host disease with a lupus-like syndrome. *J. Immunol.* 172: 1531–1539.
38. Kang, H. K., M. A. Michaels, B. R. Berner, and S. K. Datta. 2005. Very low-dose tolerance with nucleosomal peptides controls lupus and induces potent regulatory T cell subsets. *J. Immunol.* 174: 3247–3255.
39. Hahn, B. H., R. P. Singh, A. La Cava, and F. M. Ebling. 2005. Tolerogenic treatment of lupus mice with consensus peptide induces Foxp3-expressing, apoptosis-resistant, TGFbeta-secreting CD8+ T cell suppressors. *J. Immunol.* 175: 7728–7737.
40. Sharabi, A., and E. Mozes. 2008. The suppression of murine lupus by a tolerogenic peptide involves foxp3-expressing CD8 cells that are required for the optimal induction and function of foxp3-expressing CD4 cells. *J. Immunol.* 181: 3243–3251.
41. Filaci, G., S. Bacilieri, M. Fravega, M. Monetti, P. Contini, M. Ghio, M. Setti, F. Puppo, and F. Indiveri. 2001. Impairment of $CD8^+$ T suppressor cell function in patients with active systemic lupus erythematosus. *J. Immunol.* 166: 6452–6457.
42. Suzuki, M., C. Konya, J. J. Goronzy, and C. M. Weyand. 2008. Inhibitory $CD8^+$ T cells in autoimmune disease. *Hum. Immunol.* 69: 781–789.
43. Skaggs, B. J., R. P. Singh, and B. H. Hahn. 2008. Induction of immune tolerance by activation of $CD8^+$ T suppressor/regulatory cells in lupus-prone mice. *Hum. Immunol.* 69: 790–796.
44. Reynolds, J., V. A. Norgan, U. Bhambra, J. Smith, H. T. Cook, and C. D. Pusey. 2002. Anti-CD8 monoclonal antibody therapy is effective in the prevention and treatment of experimental autoimmune glomerulonephritis. *J. Am. Soc. Nephrol.* 13: 359–369.
45. Pace, L., A. Tempez, C. Arnold-Schrauf, F. Lemaitre, P. Bousso, L. Fetler, T. Sparwasser, and S. Amigorena. 2012. Regulatory T cells increase the avidity of primary $CD8^+$ T cell responses and promote memory. *Science* 338: 532–536.

JVI
Journals.ASM.org

Differential Requirements of Cellular and Humoral Immune Responses for *Fv2*-Associated Resistance to Erythroleukemia and for Regulation of Retrovirus-Induced Myeloid Leukemia Development

Sachiyo Tsuji-Kawahara, Hiroyuki Kawabata,* Hideaki Matsukuma,* Saori Kinoshita, Tomomi Chikaishi, Mayumi Sakamoto, Yuri Kawasaki, Masaaki Miyazawa

Department of Immunology, Kinki University Faculty of Medicine, Osaka-Sayama, Osaka, Japan

To assess the possible contribution of host immune responses to the exertion of *Fv2*-associated resistance to Friend virus (FV)-induced disease development, we inoculated C57BL/6 (B6) mice that lacked various subsets of lymphocytes with FV containing no lactate dehydrogenase-elevating virus. *Fv2*^{r} B6 mice lacking CD4$^+$ T cells developed early polycythemia and fatal erythroleukemia, while B6 mice lacking CD8$^+$ T cells remained resistant. Erythroid progenitor cells infected with spleen focus-forming virus (SFFV) were eliminated, and no polycythemia was observed in B cell-deficient B6 mice, but they later developed myeloid leukemia associated with oligoclonal integration of ecotropic Friend murine leukemia virus. Additional depletion of natural killer and/or CD8$^+$ T cells from B cell-deficient B6 mice resulted in the expansion of SFFV proviruses and the development of polycythemia, indicating that SFFV-infected erythroid cells are not only restricted in their growth but are actively eliminated in *Fv2*^{r} mice through cellular immune responses.

Detection of viral infection results in the activation of adaptive immune responses that clear the pathogen and provide protection against future reinfection with the same virus. The host immune system that exerts these adaptive immune responses is mainly comprised of B cells, which produce antivirus antibodies (Ab) and thus neutralize the extracellular virus, and cytotoxic T cells (CTLs), which lyse infected cells and thus restrain intracellular viral reservoirs. Many successful vaccines induce both cell- and Ab-mediated immune responses, which can last a lifetime. However, even these successful vaccines do not completely prevent infections, but rather they control viral replication upon infection and thus protect against virally induced disease development. Most HIV-infected individuals are able to mount anti-HIV immune responses, but these responses generally do not result in protection against virus replication and HIV-induced disease development (44). Therefore, additional factors are required to translate the viral detection into effective protection, as occurs in the cases of HIV elite controllers, who are able to naturally control the virus without the aid of antiretroviral drugs (13, 42). These resistant individuals have been employed to understand the mechanisms underlying protective immune responses against retrovirus infection.

We have used Friend leukemia virus (FV) infection as a model to assess the different roles of cell- and Ab-mediated immune responses in protection against retrovirus infection. Since Friend disease was first reported in 1957 (17), acute erythroleukemia induced by various strains of FV in different strains of mice has provided an excellent model to study multistage leukemogenesis, which is affected by several host factors (2, 9, 25). FV is a pathogenic retrovirus complex composed of replication-competent Friend murine leukemia virus (F-MuLV) and defective spleen focus-forming virus (SFFV). In the initial stage of FV-induced disease development, the product of the SFFV *env* gene, gp55, forms a complex with the erythropoietin receptor and the short form of the stem cell-specific receptor tyrosine kinase (Stk), and this interaction induces the growth and terminal differentiation of erythroid progenitor cells, causing increased hematocrit values and massive splenomegaly (37, 41). The late stage of Friend disease is marked by proviral integration into the *Fli1* or *PU.1* (*Sfpi1*) locus, resulting in a block of erythroid differentiation and the development of mono- or oligoclonal erythroleukemia (3, 39).

Several host genetic factors control FV replication and leukemogenesis, thus conferring resistance to FV-induced disease development (9, 37). These can be divided into a few categories based on the mechanism of resistance: the first group consists of two genes, *Fv4* and *Fv1*, the products of which directly restrict target cell entry or proviral integration of F-MuLV and SFFV (5, 23). The second group consists of host genes that influence FV-induced disease more indirectly by affecting antiviral immune responses. These include major histocompatibility complex (MHC) genes (9, 36) and a non-MHC gene, *Rfv3*. The latter has been shown to influence the duration of viremia and the production of virus-neutralizing antibodies (11, 20, 26). Recently, it was demonstrated that polymorphisms in both the apolipoprotein B mRNA-editing enzyme catalytic polypeptide-like editing complex 3 (*APOBEC3*) and BAFF receptor (BAFF-R) are associated with the levels of viremia, and the C57BL strain of mice possesses resistance alleles at both of these gene loci (32, 52, 60, 61). The third group consists of genes that influence the progression of FV-induced

Received 2 September 2013 **Accepted** 3 October 2013
Published ahead of print 9 October 2013
Address correspondence to Sachiyo Tsuji-Kawahara, skawa@med.kindai.ac.jp, or Masaaki Miyazawa, masaaki@med.kindai.ac.jp.
* Present address: Hiroyuki Kawabata, Department of Internal Medicine, Saiseikai Matsusaka General Hospital, Mie, Japan; Hideaki Matsukuma, Department of Acupuncture, Faculty of Health Sciences, Morinomiya University of Medical Sciences, Suminoe, Osaka, Japan.

doi:10.1128/JVI.02506-13

disease. Mice of the C57BL background possess a mutation in the intron of the *Stk* gene and lack the expression of the short-form Stk (sf-Stk), by which they resist the development of SFFV-induced erythroid cell proliferation and the resultant massive splenomegaly (46). This host factor was first described as the *Fv2* gene, with the resistance allele found in C57BL mice being designated as the recessive *Fv2*^{r} gene (33).

C57BL/6 (B6) mice potently resist FV-induced diseases due to their resistant genotypes at multiple loci, but the resistance is not absolute (14). Thymus-deprived B6 *nu/nu* mice develop FV-induced leukemia (28). In addition, treatment with a single dose of anti-Thy-1.2 Ab permitted the continued replication of FV in B6 mice (63). Further, B6 mice lacking either CD4$^+$ or CD8$^+$ T cells developed splenomegaly upon infection with FV containing lactate dehydrogenase-elevating virus (LDV) (19, 50). Therefore, T cell-mediated immune responses are essential for controlling FV replication and pathogenesis, even in the *Fv2*^{r} B6 background. However, it is not clear whether Ab-mediated immune responses are also required for the control of FV-induced leukemia development in B6 mice. We recently revealed that B6 mice lacking the resistance allele at the *APOBEC3* or *BAFF-R* locus show a significant delay in the initiation of virus-neutralizing Ab production and harbor more than 100 times higher numbers of virus-producing cells than do the wild-type (WT) counterparts during acute infection with FV (61). However, these mice later recovered from FV infection and never developed leukemia, indicating that at least early production of virus-neutralizing Ab is not required for resistance to FV-induced leukemia development in B6 mice. In contrast, B cells, but not CD8$^+$ T cells, were essential for protective immune responses against FV infection induced in highly susceptible *Fv2*$^{r/s}$ (C57BL/6 × BALB/c)F$_1$ (CB6F$_1$) mice by immunization with a peptide containing a single CD4$^+$ T cell epitope that was identified within the F-MuLV *env* gene product (27, 35).

To examine the possible roles of Ab-mediated immunity in controlling FV-induced leukemogenesis in the *Fv2*^{r} setting, we utilized B6 mice lacking various subsets of lymphocytes and followed the long-term consequences of lymphocyte deficiencies. The results revealed that antiretroviral Ab responses are essential for the long-term control of F-MuLV replication and for the prevention of leukemogenesis, but SFFV-infected erythroid cells are eliminated by cellular responses in the absence of B cells.

MATERIALS AND METHODS

Mice. C57BL/6NCrSlc and BALB/cCrSlc mice were purchased from Japan SLC, Inc., Hamamatsu, Japan. B6.129P2-$\beta 2m^{tm1Unc}$/J mice carrying homozygous disruption of the β_2-microglobulin gene ($\beta 2m$) were purchased from The Jackson Laboratory, Bar Harbor, ME. B6.129S2-*Ighm*^{tm1Cgm}/J mice carrying homozygous disruption of the membrane exon of the Ig μ-chain gene (μ-chain membrane exon targeted; *μMT*/*μMT*) and thus lacking B lymphocytes (29) were also purchased from The Jackson Laboratory, and BALB/c-*μMT*/*μMT* mice were established in our animal facilities by backcross mating of BALB/c mice with the B6-*μMT*/*μMT* mice (27). CB6F$_1$ mice lacking B cells were produced by crossing the B6-*μMT*/*μMT* and BALB/c-*μMT*/*μMT* mice as previously described (27). C57BR/cdJ mice, which do not express membrane-bound CD4, have been described (40). They were backcrossed to B6 mice at least nine times. Both male and female mice at 7 to 8 weeks of age were infected and followed for 20 to 24 weeks. All animals were housed and bred in the Experimental Animal Facilities at Kinki University Faculty of Medicine under specific-pathogen-free conditions, and the experiments described here have been approved by Kinki University.

Virus and inoculation. A stock of B-tropic FV complex without contamination of LDV has been described elsewhere (60). Previously used FV stocks prepared as spleen homogenates contained LDV as an unintended consequence of repeated *in vivo* passage (37, 50). Coinfection with LDV strongly suppressed FV-specific CD8$^+$ T cell responses, but FV-reactive CD4$^+$ T cell and Ab responses were not affected (50). LDV contamination was also associated with potent type I interferon responses that were not attributable to FV (18) and also polyclonal activation of both T and NK cells (37). The FV stock used here was generated *in vitro* (50), passaged in BALB/c mice for 9 days to obtain a high enough titer, and confirmed to be free of LDV by PCR assays and by the lack of polyclonal immune stimulation (37). The SFFV titer was determined by enumerating 14-day spleen foci in BALB/c mice and the F-MuLV titer by infectious focus assays on *Mus dunni* cells and with monoclonal Ab (MAb) 720 (35, 49). No infectious propagation of mink cell focus-inducing (MCF) viruses reactive with MAb 514 (8) was observed after inoculation of the FV stock onto *Mus dunni* cells. Replication-competent helper virus of FV, F-MuLV, was purified from a culture supernatant of *Mus dunni* cells persistently infected with an infectious molecular clone, FB29 (56). B6 mice were infected with 5,000 spleen focus-forming units (SFFU) of the FV stock or 5,000 focus-forming units of the FB29 stock, and FV-susceptible CB6F$_1$ mice were infected with 150 SFFU of FV. Infected mice were observed daily, and their hematocrit values were measured every 2 weeks as described previously (61).

Cell harvest and flow cytometry. Flow cytometric analyses of cell surface markers were performed as described elsewhere (59, 61). Spleen and bone marrow tissues were dissociated in phosphate-buffered balanced salt solution (PBBS) containing 2% fetal bovine serum (FBS), and a single-cell suspension was prepared by passing each dissociated tissue through a nylon mesh. Cells were incubated with anti-mouse CD16/CD32 (BD Biosciences, San Jose, CA) to prevent the test Ab from binding to Fc receptors and then stained with a combination of the following MAbs with appropriate fluorescence labeling (61): anti-mouse CD3, CD11b, CD11c, CD14, MHC class II I-E/I-A, Ly6G, and TER-119 (BD Biosciences). F-MuLV-infected cells were detected with biotinylated MAb 720 and fluorescence-conjugated streptavidin as described previously (49). The SFFV Env protein was detected with MAb 514, which also reacts with some recombinant polytropic viruses, including Friend MCF virus isolates (8), and endogenous and recombinant polytropic viruses were detected with MAb 24-6 (47). 7-Aminoactinomycin D (7-AAD) viability dye (Beckman Coulter, Inc., Brea, CA) was used to exclude dead cells. Data were acquired with a FACSCalibur and were analyzed with CellQuest Pro software (BD Biosciences).

Quantitation of proviral copy numbers. Genomic DNA was purified from spleens or bone marrow cells by using a DNeasy blood and tissue kit (Qiagen, Hilden, Germany) and treated with RNase I. Proviruses in 100 ng or 500 ng of genomic DNA were quantified by using Platinum quantitative PCR superMix-UDG with ROX (Life Technologies, Carlsbad, CA) and a Prism 7900HT real-time PCR system (Life Technologies). PCR primers and TaqMan probes for the differential detection of F-MuLV and SFFV were designed based on the *env* portion of each provirus with primers 5′-AAGTCTCCCCCCGCCTCTA-3′ and 5′-AGTGCCTGGTAAGCT CCCTGT-3′ and a 6-carboxyfluorescein (FAM)-labeled probe, 6-FAM–5′-ACTCCCACATTGATTTCCCCGTCC-3′, for the detection of F-MuLV and primers 5′-TCTAACCTCACCAACCCTGAT-3′ and 5′-TTTTAGGGCA ATGGTATGATTAAAATAA-3′ and a FAM-labeled probe, 6-FAM–5′-CCTAGTGTCTGGACCCCCCTATTACGAGG-3′ for the detection of SFFV (60). After initial incubations at 50°C for 2 min and 95°C for 10 min, 40 cycles of amplification were carried out at 95°C for 30 s and at 58°C for 1 min. A TaqMan rodent glyceraldehyde-3-phosphate dehydrogenase (GAPDH) control reagent (Life Technologies) was used as an internal control. Standard curves obtained by using plasmids containing the *env* gene of each virus as templates were linear over a range of 10 to 10^6 copies in the above reaction. The estimated melting temperature indicated that none of the above primers or probes cross-hybridized with the endoge-

nous retrovirus Emv2 sequence (GenBank accession number AC158362, position 97057 to 105700) under the above reaction conditions.

Inverse PCR and sequence analysis. Clonality of and proviral integration sites in FV-infected cells were determined by inverse PCR followed by molecular cloning and DNA sequence analysis (58, 62). Genomic DNA (2 μg) was digested with BamHI enzyme for 2 h and self-ligated with T4 ligase (TaKaRa Bio, Inc., Shiga, Japan) at 16°C overnight. The resultant circular DNA was used in the primary PCR. Amplification of the virus-host junction was performed in 50 μl of PCR buffer containing 350 μM deoxynucleoside triphosphates, 3.75 units of *Taq* DNA polymerase (Expand Long Template PCR system; Roche Diagnostics, Mannheim, Germany), and 0.3 μmol of each primer. The forward primer was designed to bind to the long terminal repeat (LTR) regions of both proviruses, and the reverse primers were specific for the *env* portion of each provirus, as follows: common forward primer, 5′-CCAAGGACCTGAAATGACCCTG-3′; reverse primer specific for F-MuLV, 5′-GACTTGGCAGGTTTGGGT AGG-3′; reverse primer specific for SFFV, 5′-GAGGAGGTGGGGCAGT CTCG-3′. PCR amplification was carried out in an iCycler thermal cycler (Bio-Rad Lab, Tokyo, Japan) under the following conditions: the first step was 15 cycles at 92°C for 10 s, 59°C for 30 s, and 68°C for 8 min, preceded by an initial denaturation at 92°C for 2 min; the second step was 20 cycles at 92°C for 10 s, 59°C for 30 s, and 68°C for 8 min, with a 20-s extension of the elongation step for each successive cycle, followed by a final extension at 68°C for 7 min. The PCR products were separated by agarose gel electrophoresis and stained with ethidium bromide. Separated DNA bands with a length of more than 25 bp were purified using a Wizard PCR Preps DNA purification system (Promega KK, Tokyo, Japan) and subcloned into the pCR2.1-TOPO or pCRXL-TOPO (Life Technologies) plasmid. Sequence analysis was performed by using a primer located in the LTR, 5′-GAGCTCACAACCCCTCACTC-3′. Database analysis of the obtained sequences was performed by using the BLASTN homology search program provided by the National Center for Biotechnology Information (http://www.ncbi.nlm.nih.gov/), and proviral integration sites were determined. When proviruses were integrated outside of a previously identified gene locus, the distances between the integrated provirus and the nearest gene were calculated. To determine proviral sequences within genomic DNA prepared from spleens of B cell-deficient B6 mice, the 3′ *env*-LTR portions of F-MuLV proviruses were amplified from 200 ng of genomic DNA by PCR using the following primers: forward primer specific for the *env* portion of F-MuLV, 5′-AAGTCTCCCCCCGCCTCTA-3′; reverse primer for the LTR region, 5′-AAGGCACAGGGTCATTTCA GGTC-3′. The amplified PCR products were separated by agarose gel electrophoresis, and their lengths were measured.

Cell morphology. Single-cell suspensions were prepared from the spleens as described above. Cytospin preparations of the spleen cells and peripheral blood smear specimens were stained with May-Grunwald Giemsa stain.

Infectious center assays. Infectious center assays were performed as described previously (27, 35). Briefly, spleen and bone marrow cell suspensions prepared from mice challenged with F-MuLV were serially diluted with PBBS containing 2% FBS, plated in triplicate at concentrations between 10^3 and 10^6 cells per well of 24-well plates onto monolayers of *Mus dunni* cells that had been seeded at 1×10^4 cells per well on the previous day, and cocultured for 2 days. To ensure the lack of detectable virus-producing cells, 6×10^7 spleen cells and 3×10^7 bone marrow cells from each mouse were plated in 20 and 10 wells of 24-well plates, respectively, at a concentration of 3×10^6 cells per well. After fixation with methanol, cocultured *Mus dunni* cells were stained with biotinylated MAb 720, 514, 24-6, or 24-8 (8, 47, 49), and foci were visualized by using the avidin-biotinylated peroxidase complex (Vector Laboratories, Burlingame, CA) and counted under a magnifier.

Cell depletion *in vivo*. NK cells were depleted as described previously (24, 43). Briefly, rabbit antiserum specific for mouse asialo-ganglio-*N*-tetraosylceramide (asialoGM1) and control normal rabbit serum were purchased from Wako Pure Chemicals (Osaka, Japan), and the IgG fraction was concentrated by precipitation with 45% (final concentration) ammonium sulfate. Mice were injected intravenously with 60 μg/dose of the anti-asialoGM1 Ab 1 day prior to FV inoculation and 2, 5, 8, 11, 14, 21, and 28 days after virus infection. $CD8^+$ T cells were depleted by injecting anti-mouse CD8 (Lyt-2.2) MAb. The rat anti-mouse CD8 MAb was purified from the culture supernatant of hybridoma 2.43 cells (American Type Culture Collection, Manassas, VA) as described previously (51). Mice were intravenously given a 200 μg/dose of the purified anti-CD8 MAb at 7, 3, and 1 day prior to FV inoculation and 1, 2, and 3 weeks after virus inoculation. Rat IgG was given to the control group.

Statistical analyses. One-way or two-way analyses of variance (ANOVA) and Mantel-Cox tests of survival curves were performed by using Prism software (GraphPad Software, Inc., San Diego, CA) with indicated posttests. The Mann-Whitney test was used for non-Gaussian distributions, with Bonferroni's *post hoc* test for multiple comparisons.

RESULTS

Development of distinctive fatal pathologies upon FV infection in *Fv2*^{r} B6 mice lacking $CD4^+$ T or B lymphocytes. To investigate the possible involvement of various immune cell populations in controlling FV-induced leukemogenesis in *Fv2*^{r} mice, B6 mice lacking a specific subset of immune cells were utilized: cell membrane CD4-defective mutant mice lack $CD4^+$ T cells, cell membrane IgM-deficient *μMT/μMT* mice, which have no peripheral mature B cells, and *β2m* knockout mice, which are deficient in peripheral $CD8^+$ T cells (29, 30, 40). It has been shown that B6 mice lacking either $CD8^+$ or $CD4^+$ T cells develop splenomegaly within 6 to 10 weeks after FV infection, while most B cell-deficient B6 mice do not develop splenomegaly (19). However, the above experiment was performed by using an FV stock that contained LDV, which caused severe immune dysfunction that rendered B6 mice less resistant to FV infection (50). Further, the development of FV-induced disease takes multiple steps (25, 37, 38), which may require a longer observation period to fully assess the role of immune cell subsets, especially in highly resistant B6 mice. Therefore, we used LDV-free FV and performed more detailed cellular and molecular analyses in a long-term setting.

To study the kinetics of FV-induced disease development, we first analyzed the changes in hematocrit values and survival rates after FV inoculation in B6 mice lacking $CD4^+$ or $CD8^+$ T cells or B lymphocytes. All of the WT B6 mice survived for 20 weeks after FV inoculation, confirming that B6 mice are highly resistant to FV infection (Fig. 1). However, 80 to 95% of B6 mice deficient for either $CD4^+$ T or B cells died within 8 to 20 weeks after FV infection, with significantly shorter survival periods than infected WT mice ($P = 0.01$ and $P = 0.0003$, respectively). In contrast, only a small fraction of mice lacking $CD8^+$ T cells died upon FV inoculation, and their survival rate was not different from that of WT mice ($P > 0.48$). As for the hematocrit values, none of the WT B6 mice showed polycythemia upon FV infection, whereas only one mouse in the $CD8^+$ T cell-deficient group showed a decrease in hematocrit values just before its death, and none showed polycythemia (Fig. 2A). On the other hand, most of the $CD4^+$ T cell-deficient mice developed progressive polycythemia starting around 5 weeks postinfection or earlier. Most of these mice showed a sharp decline in hematocrit values just before death. Spleen sizes at the time of death in $CD4^+$ T cell-deficient mice were significantly larger than those in the infected WT mice (Fig. 2B). Intriguingly, the hematocrit values of B cell-deficient mice were slightly decreased but never increased upon FV infection (Fig. 2A). Nevertheless, in a long-term follow-up experiment, B

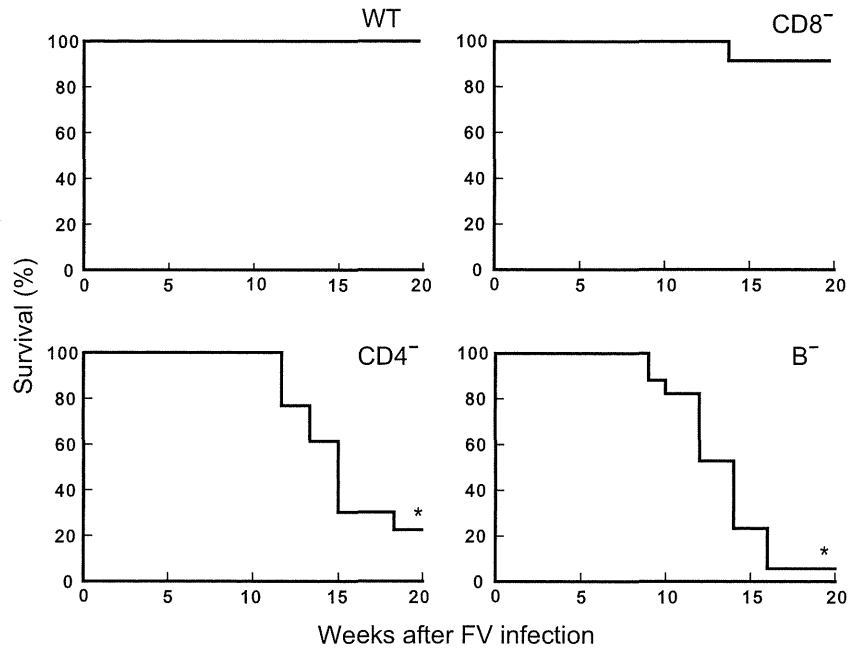

FIG 1 Survival of immunodeficient B6 mice upon FV infection. B6 mice lacking $CD4^+$ T cells ($CD4^-$, $n = 13$), $CD8^+$ T cells ($CD8^-$, $n = 12$), or B cells (B^-, $n = 17$) and wild-type B6 mice ($n = 11$) were inoculated with 5,000 SFFU of FV, and their survival was monitored for 20 weeks. *, significantly different from the survival curve of the WT mice based on the Mantel-Cox test. The entire set of experiments was repeated with >10 mice for each group, and essentially the same results were obtained.

cell-deficient B6 mice died more rapidly than the $CD4^+$ T cell-deficient mice that showed massive polycythemia in the earlier stage (Fig. 1; $P = 0.001$). Consistent with the lack of increases in their hematocrit values, spleen weights of B cell-deficient B6 mice at around the day of their death were only slightly higher than those of the infected WT mice (Fig. 2B). These results indicate that $CD4^+$ T cells are indispensable for the control of FV-induced erythroid cell proliferation and the resultant development of fatal leukemia, while $CD8^+$ T cells are not required, contrary to the previous results obtained with the LDV-containing FV (19). Fur-

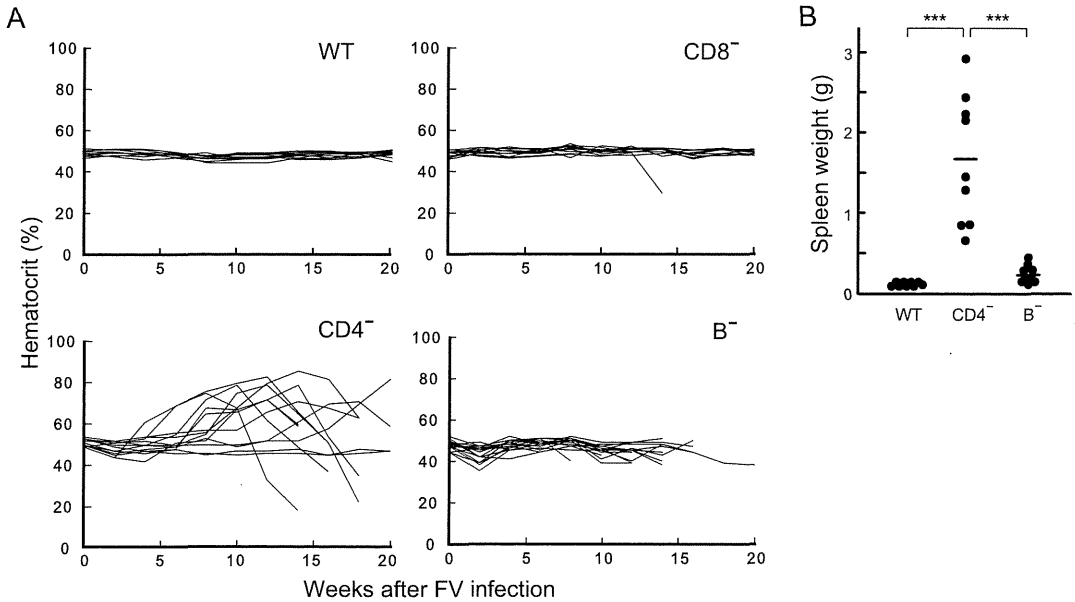

FIG 2 Changes in hematocrit values and spleen weights in FV-infected B6 mice. B6 mice lacking $CD4^+$ T cells ($CD4^-$, $n = 13$), $CD8^+$ T cells ($CD8^-$, $n = 12$), or B cells (B^-, $n = 17$) and WT B6 mice ($n = 11$) were inoculated with 5,000 SFFU of FV. (A) Hematocrit values were measured every 2 weeks after FV inoculation. Each line shows the time-dependent changes in hematocrit values in each individual mouse. (B) Spleen weights were measured at around the day of death or at 20 weeks postinfection for surviving mice. Each circle shows the actual weight of the spleen of an individual mouse, and horizontal bars represent the mean values for each group. Note that some mice died before the measurement of spleen weight, and thus not all individuals in panel A are included. ***, $P < 0.001$ by one-way analysis of variance with Tukey's *post hoc* test for multiple comparisons. Similar data were obtained in two separate experiments.

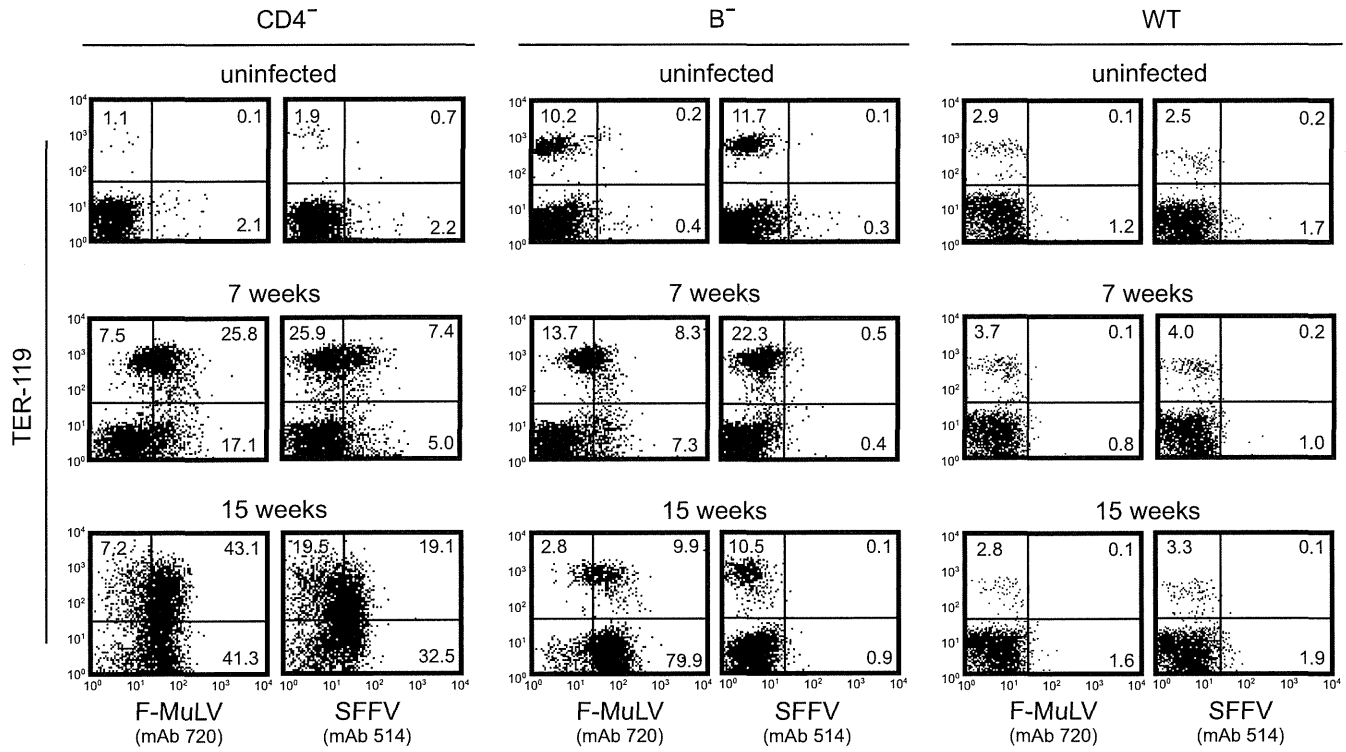

FIG 3 Changes in the proportions of F-MuLV- and SFFV-infected erythroid cells in the spleens of $CD4^+$ T cell- or B cell-deficient B6 mice. Spleen cells were prepared from B6 mice lacking $CD4^+$ T cells ($CD4^-$) or B cells (B^-) and from WT B6 mice before or at 7 or 15 weeks after FV inoculation and were stained with MAb 720 or 514 as well as the MAb specific for TER-119, a marker for late erythroid lineage cells. Representative dot plots are shown. The value in each quadrant indicates the percentage of cells that expressed the indicated marker.

ther, B cells are not required to control FV-induced erythroid cell proliferation, but FV induces a fatal disease in the absence of B cells without causing massive splenomegaly.

SFFV becomes undetectable in B cell-deficient B6 mice after FV infection. In order to address why FV-induced polycythemia was observed in $CD4^+$ T cell-deficient, but not in B cell-deficient, B6 mice, we first analyzed the expansion and differentiation of virus-infected erythroblasts and copy numbers of F-MuLV and SFFV proviruses in the spleens of B6 mice deficient for each type of the immune cells. MAb 720 exclusively detects the *env* gene product of F-MuLV, whereas MAb 514 reacts with the polytropic virus-derived portion of the SFFV and recombinant MCF virus Env proteins, but not with ecotropic, xenotropic, or amphotropic viruses (8, 49). In the spleens of $CD4^+$ T cell-deficient mice, TER-119^+ terminally differentiating erythroid cells massively expanded with time after FV inoculation. These cells also expressed both F-MuLV Env gp70 and SFFV Env gp55 (Fig. 3). Consistent with these observations, the copy numbers of both proviruses markedly increased in the spleens of $CD4^+$ T cell-deficient animals (Fig. 4A and B). On the contrary, in B cell-deficient B6 mice, 514^+ SFFV-infected cells were hardly detectable by flow cytometry, and the percentages of erythroid cells were only slightly increased at 7 weeks after FV infection, while F-MuLV $gp70^+$ cells were readily detected and increased with time (Fig. 3). Note that, due to the lack of B cells, percentages of TER-119^+ erythroid cells in $\mu MT/\mu MT$ mice were higher than those in WT mice even before FV infection. Similarly, in the quantitative analysis of proviral copy numbers, SFFV provirus was barely detectable in the B cell-deficient mice at 2 weeks after FV inoculation and became undetectable by 7 weeks postinfection, whereas the copy numbers of F-MuLV provirus increased over time (Fig. 4A and B). As expected, small numbers of F-MuLV proviruses were detectable at 2 weeks postinfection, but both proviruses became undetectable in the WT B6 mice by 15 weeks after FV inoculation.

As SFFV proviruses and cells reactive with MAb 514 were both barely detectable despite a high dose of FV inoculation, we asked if SFFV fails to replicate or if SFFV-infected cells are selectively eliminated from the spleens of B cell-deficient B6 mice. One possible explanation for the lack of SFFV provirus detection in B cell-deficient B6 mice is that B cells are required for the propagation of SFFV. To examine this possibility, $CB6F_1$ mice without *Fv2*-associated resistance ($Fv2^{r/s}$) and lacking B cells were infected with a low dose of FV complex. In B cell-deficient $CB6F_1$ mice, SFFV proviruses were detectable in the spleen of 1 of the 3 animals tested as early as 1 week after FV inoculation, and significantly high copy numbers were detected 2 weeks postinfection in all tested animals despite the low inoculum dose (Fig. 4C), indicating that SFFV can replicate in the absence of B cells. In fact, B cell-deficient $CB6F_1$ mice showed moderate splenomegaly at 2 weeks after FV infection (average spleen weight, 0.20 ± 0.03 g [mean ± standard error of the mean; $n = 10$], compared to 0.07 to 0.10 g in uninfected $\mu MT/\mu MT$ mice of the same background), and their spleens became significantly larger (0.76 ± 0.16 g; $n = 8$) as early as 3 weeks after infection.

It has been shown that FV initially infects target cells in the bone marrow, and infectious center cells then migrate to the

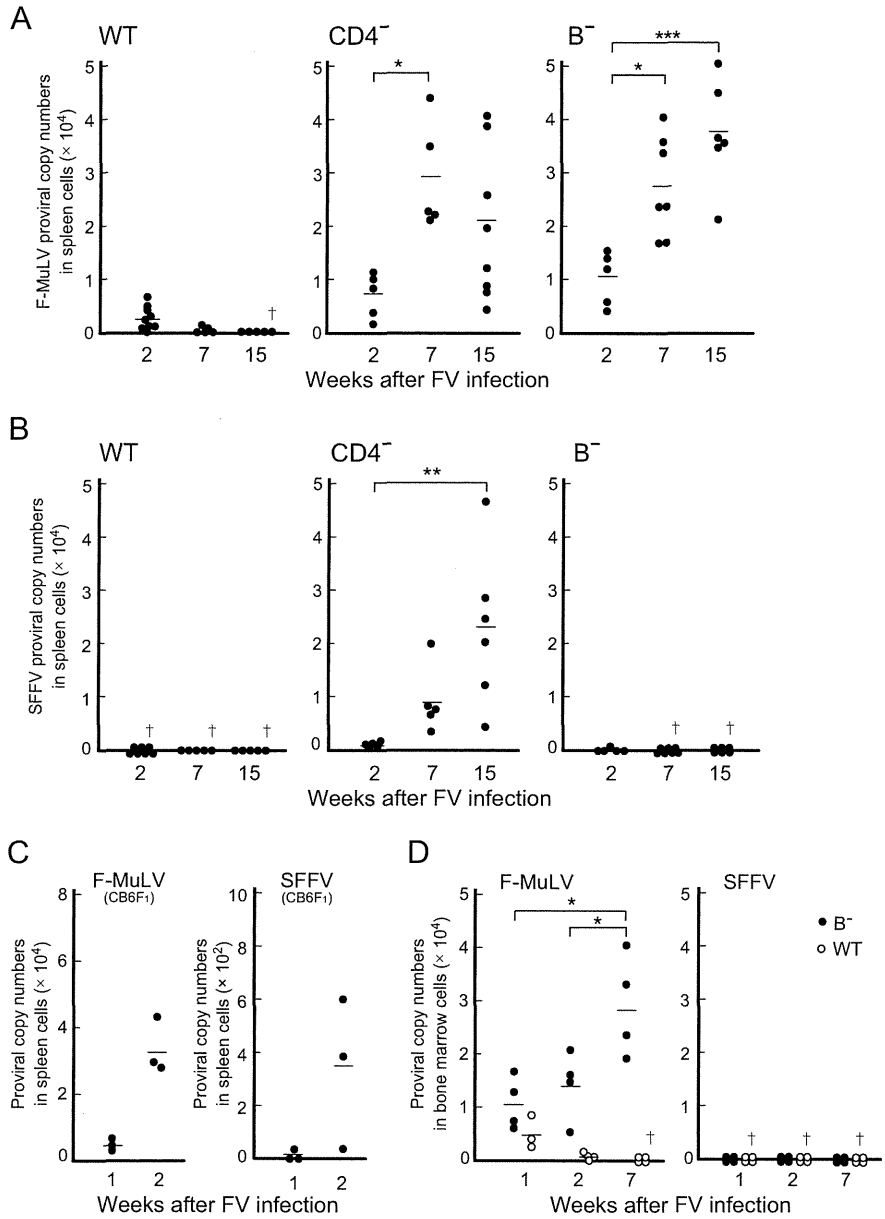

FIG 4 Kinetic changes in proviral copy numbers in FV-infected B6 or $CB6F_1$ mice. Each circle represents the actual proviral copy number detected from an individual mouse, and horizontal bars represent the mean values for each group. The FV stock inoculated contained about the same number of infectious units of F-MuLV and SFFV. (A and B) Spleen cells were prepared from WT, $CD4^+$ T cell-deficient ($CD4^-$), or B cell-deficient (B^-) B6 mice at 2, 7, and 15 weeks after FV inoculation, and the genomic DNA was obtained from the spleens. Copy numbers of either F-MuLV (A) or SFFV (B) proviruses integrated into 100 ng of spleen genomic DNA (equal to about 1.7×10^4 cells) were determined by the real time-PCR method. *, significant increase in comparison with relevant copy numbers at 2 weeks after infection ($P < 0.05$) based on a one-way analysis with Dunnett's *post hoc* test for multiple comparisons; **, $P < 0.01$; ***, $P < 0.001$; †, undetectable in all animals examined. (C) B cell-deficient $CB6F_1$ mice were inoculated with 150 SFFU of FV, and their spleen cells were prepared at 1 or 2 weeks postinfection. The copy numbers of each provirus integrated into spleen genomic DNA (100 ng) were analyzed. (D) Bone marrow cells were prepared from B cell-deficient (●) or WT (○) B6 mice at 1, 2, and 7 weeks after FV inoculation, and the proviral copy numbers in 500 ng of the bone marrow genomic DNA (equal to about 8.5×10^4 cells) were analyzed. *, significant changes in copy numbers were observed between the indicated time points ($P < 0.05$), based on a one-way analysis of variance with Tukey's *post hoc* test for multiple comparisons; †, undetectable in all animals examined.

spleen and induce stress erythropoiesis, ultimately causing splenomegaly (57). Thus, we next examined if SFFV proviruses were detectable in the bone marrow in B6 mice. As expected, F-MuLV proviruses were transiently detected in the bone marrow of WT B6 mice but quickly became nearly undetectable by 2 weeks after infection (Fig. 4D). On the other hand, F-MuLV proviruses were detectable by 1 week at higher levels and increased copy numbers through 2 to 7 weeks after infection in B cell-deficient B6 mice. Nevertheless, SFFV proviruses were not detectable even in the bone marrow of $Fv2^r$ B6 mice irrespective of B cell proficiency or deficiency. As SFFV proviruses were detected and increased in B6 mice in the absence of $CD4^+$ T cells (Fig. 4B), these data collectively indicate the possibility that SFFV is commonly eliminated in WT and B cell-deficient B6 mice as rapidly as 2 weeks after

FV infection, but B6 mice lacking $CD4^+$ T cells fail to eliminate SFFV and as a result develop massive splenomegaly and polycythemia.

Cytotoxic cells are required for early elimination of SFFV in *Fv2*^{r} B6 mice. As SFFV expanded in *Fv2*^{r} B6 mice in the absence of $CD4^+$ T cells but SFFV-infected cells and SFFV proviruses were undetectable or barely detectable at 2 weeks after FV infection in both WT and B cell-deficient B6 mice, it is possible that cellular, but not humoral, immune responses under the control of $CD4^+$ T cells may be required for early elimination of SFFV-infected cells. In fact, it has been shown that NK cells are required for immune control of FV-induced disease development that is brought about by priming $CD4^+$ T cells with a peptide vaccine (24), and NK cells directly recognize and control the expansion of FV-infected erythroid cells (43). Therefore, to explore the presumable roles of cytotoxic effector cells on the elimination of SFFV-infected cells, we administered Ab specific to asialoGM1, CD8, or both to B cell-deficient B6 mice and depleted the numbers of NK and/or $CD8^+$ cells. In B cell-deficient B6 mice depleted of either NK or $CD8^+$ cells or both NK and $CD8^+$ cells, polycythemia was observed after FV infection (Fig. 5A). More importantly, the analyses of proviral copy numbers in the late phase of FV infection also showed that SFFV proviruses became detectable in the spleens of B cell-deficient B6 mice upon depletion of $CD8^+$ and/or NK cells (Fig. 5B), although the copy numbers of SFFV provirus were lower than in $CD4^+$ T cell-deficient B6 mice (Fig. 4B). Furthermore, at earlier time points after FV infection, SFFV proviruses also became detectable in B cell-deficient B6 mice after injection with both anti-CD8 and anti-asialoGM1 Ab, while F-MuLV copy numbers were not significantly affected by Ab injections (Fig. 5C), indicating that SFFV-infected cells are indeed selectively eliminated, at least in part, by $CD8^+$ T cells and/or NK cells in the very early phase of FV infection in B6 mice lacking B cells. Taken together, these results indicate that, in FV-infected B cell-deficient B6 mice, SFFV was not detectable because SFFV-infected cells were eliminated by cellular immune responses exerted at least partly by NK and/or $CD8^+$ T cells.

F-MuLV alone, but not SFFV, is responsible for the deaths of B cell-deficient B6 mice. As B cell-deficient B6 mice died without signs of either polycythemia or massive splenomegaly, we next asked if the pathogenic process after FV infection is different between $CD4^+$ T cell- versus B cell-deficient B6 mice. To this end, we first detected proviral integration sites in the spleen by using the inverse PCR method and determined the clonality of cells harboring the proviruses. At 7 weeks postinfection, numerous different integration sites for F-MuLV proviruses were found in the spleens of both $CD4^+$ T cell- and B cell-deficient B6 mice, reflecting the polyclonal nature of FV-infected cells (Fig. 6). Consistent with the results of flow cytometry and real-time PCR analyses, SFFV proviral integration into the spleen cell genome was not detected in B cell-deficient mice. In contrast, limited numbers of FV integration sites were observed at 15 weeks postinfection in both strains of mice, indicating the emergence of transformed leukemic clones. Again, oligoclonal integration of F-MuLV alone was observed in B cell-deficient B6 mice. In addition, to analyze proviral sequences in the genomic DNA purified from B cell-deficient B6 mice, the 3′ *env*-LTR fragments of F-MuLV provirus were directly amplified in PCR assays. The sizes of amplified DNA fragments were all identical to that of F-MuLV provirus (data not shown), ruling out the possible insertion of endogenous retroviral sequences into the amplified segment. Taken together, these results suggest that the FV-induced mortality observed in B cell-deficient B6 mice might be caused by leukemia associated with persistent replication of F-MuLV.

Inoculation of F-MuLV alone is sufficient to induce fatal disease in adult B6 mice when B cells are lacking. F-MuLV free of SFFV has been shown to induce leukemia when inoculated into newborn mice of susceptible strains (10, 54, 55). However, our results, described in the above sections, strongly indicated that F-MuLV alone in the absence of SFFV replication induced a fatal disease with oligoclonal expansion of largely TER-119^- cells in B cell-deficient adult B6 mice. Thus, we next asked if inoculation of F-MuLV free of SFFV into adult B6 mice induced a similar pathology in the absence of B cells. In fact, most of the B cell-deficient B6 mice died after inoculation of F-MuLV alone, while their hematocrit values were not increased until death (Fig. 7). This indicated that F-MuLV in the absence of SFFV is sufficient to induce the fatal pathology in B cell-deficient B6 mice. Therefore, we next investigated whether the fatal pathology observed in B cell-deficient B6 mice was caused by the persistent infection with F-MuLV itself or through the generation of recombinant MCF viruses and their insertion into the host cell genome. To detect the possible presence of recombinant MCF viruses, we performed infectious center assays with three MAbs that reacted with known recombinant MCF viruses (8, 47). In the spleen and bone marrow prepared from B cell-deficient B6 mice between 14 and 17 weeks after F-MuLV infection, no recombinant MCF viruses were detectable by any of these MAbs (Fig. 8), while F-MuLV was readily detected. Even when as many as 6×10^7 and 3×10^7 cells prepared from the spleen and bone marrow, respectively, were seeded as infectious centers, no foci were detectable with the above MCF-reactive MAbs. Further, in fluorescence-activated cell sorter analyses performed at 7 and 15 weeks after infection, spleen cells in FV-infected, B cell-deficient B6 mice were not only negative for MAb 514 (Fig. 3), but also were negative for cell surface binding of MAb 24-6, which is known to react with representative FV MCF isolates (data not shown) (47). Thus, the fatal pathology was most likely induced by persistent infection by F-MuLV itself, and not through the emergence of infectious MCF viruses in B6 mice lacking B cells.

Development of myeloid leukemia in FV- or F-MuLV-infected B6 mice lacking B cells. In the analyses of provirus integration sites by use of the inverse PCR method, oligoclonal expansion of F-MuLV-infected cells was observed in the spleens of B cell-deficient B6 mice in the late phase of FV infection (Fig. 6), suggesting presumable leukemia development in these mice as the cause of the observed fatality (Fig. 1). To explore whether the fatal outcome observed in B6 mice lacking B cells was caused by the development of leukemia after persistent F-MuLV infection, we next compared cellular phenotypes in the spleen as well as peripheral blood of B6 mice lacking $CD4^+$ T or B cells under pathological conditions after FV infection. In most of the $CD4^+$ T cell-deficient B6 mice under pathological conditions after FV infection, expansion of various stages of erythroblast-like cells was observed in their spleens, with the appearance of immature erythroid progenitor cells in the peripheral blood (Fig. 9A), similar to those changes observed in FV-susceptible mice possessing the *Fv2*^{s} allele after FV infection. The low- to medium-level expression of TER-119 on the $gp70^+$ cells expanded in the spleen was demonstrated by flow cytometry in cells from the majority of $CD4^+$ T cell-deficient B6

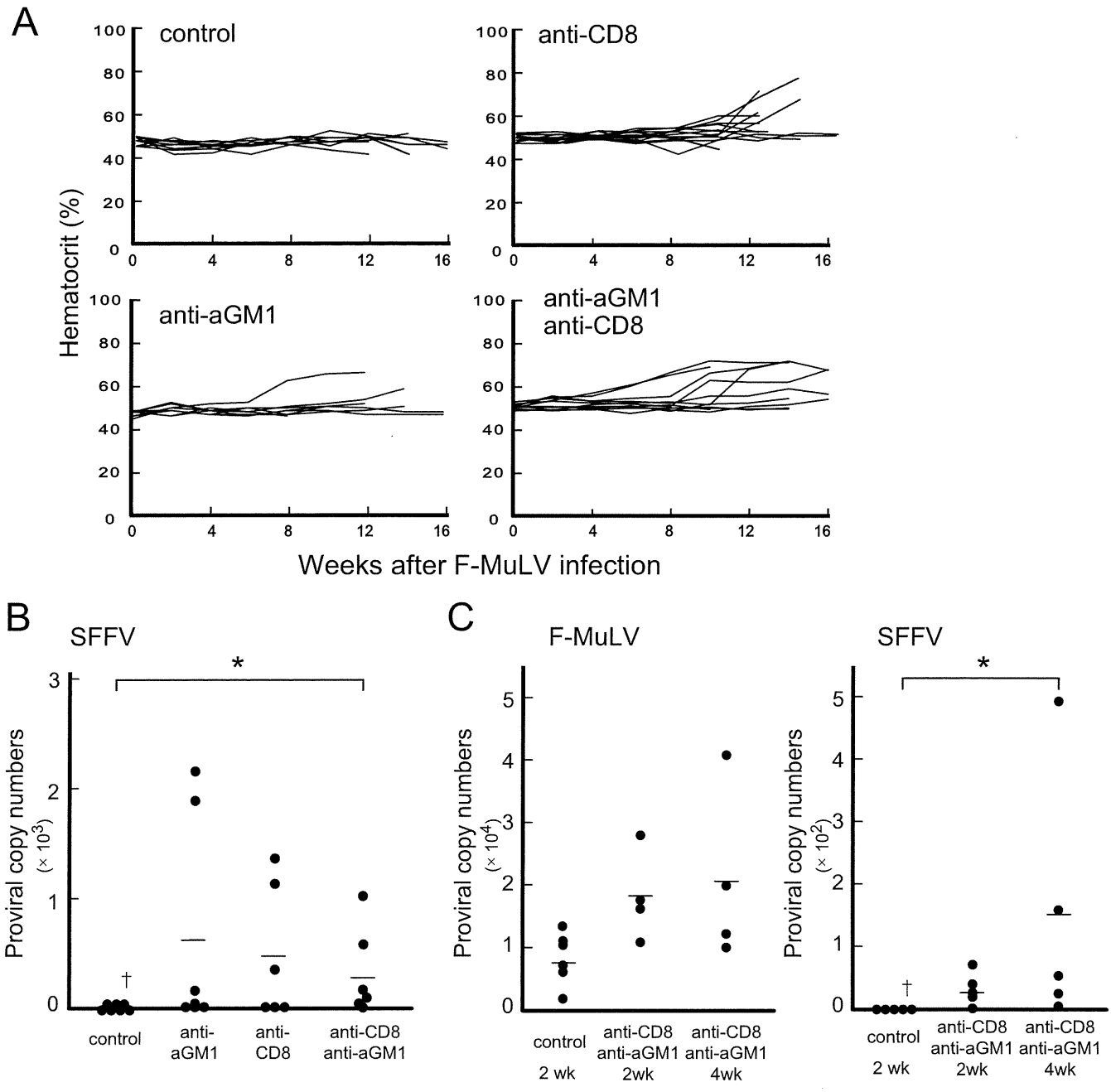

FIG 5 Roles of CD8$^+$ T and NK cells in the regulation of SFFV-infected cell expansion in B cell-deficient B6 mice. B cell-deficient B6 mice were injected with anti-mouse CD8 and/or anti-asialoGM1 (aGM1) Ab and inoculated with 5,000 SFFU of FV. Control mice were injected with a mixture of normal rabbit and normal rat sera before FV infection. (A) Changes in hematocrit values in B cell-deficient mice depleted of CD8$^+$ T (n = 15), NK (n = 10), or both types of cells (n = 12) or in those given the control sera (n = 9). Each line shows time-dependent changes in hematocrit values in each individual mouse. (B) Copy numbers of SFFV proviruses in spleen genomic DNA (100 ng) prepared from B cell-deficient B6 mice depleted of CD8$^+$ T, NK, or both types of cells. The mice were analyzed at 12 to 16 weeks postinfection. †, undetectable in all animals examined; *, significantly different in copy numbers in comparison with the control group [$P = 0.0056 < \alpha_3(0.05) = 0.017$ by Mann-Whitney test for non-Gaussian distributions with Bonferroni's *post hoc* test for multiple comparisons]. (C) Copy numbers of F-MuLV and SFFV proviruses in spleen genomic DNA (100 ng) of B cell-deficient B6 mice depleted of both CD8$^+$ T and NK cells at 2 and 4 weeks after FV inoculation. Each circle represents the actual proviral copy number detected from each individual mouse, and horizontal bars indicate the mean values for each group. †, undetectable in all animals examined; *, significantly different in copy numbers in comparison with the control group [$P = 0.0075 < \alpha_3(0.05) = 0.017$ by Mann-Whitney test for non-Gaussian distributions with Bonferroni's *post hoc* test for multiple comparisons].

mice under FV-induced pathology (Fig. 9B), confirming the erythroid nature of leukemic cells. The expansion of lymphoid cells expressing CD3 was observed in 1 of the 10 infected CD4$^+$ T cell-deficient mice examined (data not shown), indicating occasional development of lymphoid leukemia. On the other hand, large myeloid-like cells with cleaved nuclei expanded in the spleens of B cell-deficient B6 mice upon FV infection associated with vastly increased numbers of granulocytes with hypersegmented nuclei in the peripheral blood (Fig. 9A). Further, we found the expression of CD11b, Ly6G, and F-MuLV gp70, but not